

A survey of Sierra Nevada magmatism using Great Valley detrital zircon trace-element geochemistry: View from the forearc

Kathleen DeGraaff Surpless¹, Diane Clemens-Knott², Andrew P. Barth³, and Michelle Gevedon⁴

¹DEPARTMENT OF GEOSCIENCES, TRINITY UNIVERSITY, SAN ANTONIO, TEXAS 78212, USA

²DEPARTMENT OF GEOLOGICAL SCIENCES, CALIFORNIA STATE UNIVERSITY–FULLERTON, FULLERTON, CALIFORNIA 92831, USA

³DEPARTMENT OF EARTH SCIENCES, INDIANA UNIVERSITY–PURDUE UNIVERSITY INDIANAPOLIS, INDIANAPOLIS, INDIANA 46202, USA

⁴JACKSON SCHOOL OF GEOSCIENCES, THE UNIVERSITY OF TEXAS AT AUSTIN, AUSTIN, TEXAS 78712, USA

ABSTRACT

The well-characterized Sierra Nevada magmatic arc offers an unparalleled opportunity to improve our understanding of continental arc magmatism, but present bedrock exposure provides an incomplete record that is dominated by Cretaceous plutons, making it challenging to decipher details of older magmatism and the dynamic interplay between plutonism and volcanism. Moreover, the forearc detrital record includes abundant zircon formed during apparent magmatic lulls, suggesting that understanding the long-term history of arc magmatism requires integrating plutonic, volcanic, and detrital records. We present trace-element geochemistry of detrital zircon grains from the Great Valley forearc basin to survey Sierra Nevada arc magmatism through Mesozoic time. We analyzed 257 previously dated detrital zircon grains from seven sandstone samples of volcanogenic, arkosic, and mixed compositions deposited ca. 145–80 Ma along the length of the forearc basin. Detrital zircon trace-element geochemistry is largely consistent with continental arc derivation and shows similar geochemical ranges between samples, regardless of location along strike of the forearc basin, depositional age, or sandstone composition. Comparison of zircon trace-element data from the forearc, arc, and retroarc regions revealed geochemical asymmetry across the arc that was persistent through time and demonstrated that forearc and retroarc basins sampled different parts of the arc and therefore recorded different magmatic histories. In addition, we identified a minor group of Jurassic detrital zircon grains with oceanic geochemical signatures that may have provenance in the Coast Range ophiolite. Taken together, these results suggest that the forearc detrital zircon data set reveals information different from that gleaned from the arc itself and that zircon compositions can help to identify and differentiate geochemically distinct parts of continental arc systems. Our results highlight the importance of integrating multiple proxies to fully document arc magmatism, demonstrating that detrital zircon geochemical data can enhance understanding of a well-characterized arc, and these data may prove an effective means by which to survey an arc that is inaccessible and therefore poorly characterized.

LITHOSPHERE, v. 11, no. 5, p. 603–619; GSA Data Repository Item 2019264 | Published online 27 June 2019

<https://doi.org/10.1130/L1059.1>

INTRODUCTION

The well-exposed and intensely studied Sierra Nevada magmatic arc of California offers an unparalleled opportunity to understand continental arc magmatism. More than 100,000 km² of granitoid rocks now exposed in California form a composite batholith that represents the roots of eroded latest Permian through Cretaceous stratovolcanoes and arc-related edifices. Igneous rocks and associated cumulates formed a vertical lithospheric column >100 km thick in the Sierra Nevada (Saleeby et al., 2003), of which current exposure provides only partial windows.

Extensive geochemical, structural, and isotopic study has documented the evolution of Permian–Triassic through Cretaceous Sierran magmatism (e.g., Schweickert and Cowan, 1975; DePaolo, 1981; Chen and Moore, 1982; Dodge et al., 1982; Kistler et al., 1986; Saleeby et al., 1987; Chen and Tilton, 1991; Bateman, 1992; Ducea, 2001; Barth et al., 2011; Lackey et al., 2012; Cecil et al., 2012; Chapman et al., 2015; Saleeby and Dunne, 2015). Bedrock zircon and intra-arc detrital zircon studies have indicated

three episodes of high-flux magmatism in the Sierra Nevada, with magmatic pulses in Triassic, Middle and Late Jurassic, and mid-Cretaceous time, separated by two periods of low magmatic flux in Early Jurassic and Early Cretaceous time (Fig. 1; e.g., Paterson and Ducea, 2015). This chronologic record of Sierran magmatism preserved in modern exposures is necessarily partial, given that much of the associated volcanic cover has been eroded, while the deeper, unexhumed portions of the arc remain inaccessible; in fact, more than 80% of the surface area of batholithic rock is Cretaceous in age (Saleeby and Dunne, 2015). Thus, modern surface exposure of the Sierra Nevada magmatic arc is not representative of the full magmatic history of the arc, making it challenging to decipher details of older magmatism as well as the dynamic interplay between plutonism and volcanism.

Zircon has long been used for U-Th-Pb geochronology, and zircon age distributions are the primary means used to determine the timing and duration of magmatic flare-ups or relative quiescence in arcs. With the advent and expansion of secondary ion mass spectrometry (SIMS) and

laser-ablation techniques for single-grain and single-domain analyses of zircon, increasing attention to the geochemical composition of zircon, particularly with respect to concentrations of U, Th, Hf, Y, Nb, Sc, and rare earth elements (REEs), has helped researchers better interpret in situ isotopic ages, understand petrogenetic processes (e.g., Hoskin and Ireland, 2000; Hoskin and Schaltegger, 2003; Grimes et al., 2007; Claiborne et al., 2010; Grimes et al., 2015; Kirkland et al., 2015; Barth et al., 2017), and estimate parent-rock or parent-melt trace-element concentrations (e.g., Hoskin and Ireland, 2000; Sano et al., 2002; Chapman et al., 2016). Grimes et al. (2007) developed geochemical discriminant diagrams for zircon that differentiate continental and ocean crust zircon based on U/Yb and Yb, Hf, and Y concentrations. Grimes et al. (2015) refined these diagrams with an additional focus on Nb and Sc to discriminate mid-ocean ridge, plume-influenced ocean island, and subduction-related arc environments. Barth et al. (2013) demonstrated that the average retroarc detrital zircon composition is in agreement with the average in situ zircon suites for the three magmatic flare-ups of the Sierran arc, and that trace-element geochemistry in zircon records systematic changes in melt compositions through time.

Studies of Sierran arc magmatism have focused largely on the plutonic record (e.g., Stern et al., 1981; Chen and Moore, 1982; Bateman, 1992; Coleman and Glazner, 1997), but most studies of modern arcs focus on the volcanic portion as representative of magmatism (e.g., Ducea et al., 2015); only a few studies of arc magmatism focus on the detrital record (e.g., Gill et al., 1994; Arculus et al., 1995; Draut and Clift, 2013). Here, we present trace-element geochemistry of detrital zircon from the Great Valley forearc basin to survey Sierra Nevada arc magmatism through Mesozoic time, and to compare forearc and retroarc detrital zircon records of Sierran arc magmatism. We analyzed 257 previously dated detrital zircon grains from seven sandstone samples deposited ca. 145–80 Ma along the length of the forearc basin and compared the detrital zircon trace-element geochemistry with published zircon geochemistry from the retroarc region (Barth et al., 2013) and the plutonic arc (Barth et al., 2012, 2018), supplemented with new plutonic zircon data (this study). Detrital zircon grains were separated from sandstone samples with volcanogenic, arkosic (i.e., having plutonic provenance), and mixed compositions; thus, our data set provides a detrital zircon geochemical record of Sierran volcanic and plutonic arc magmatism.

A comparison of our detrital zircon data set with zircon trace-element data from the Sierra Nevada and the retroarc region revealed geochemical asymmetry across the arc that persisted through time. We documented two zircon geochemical populations that demand two different kinds of provenance in close proximity throughout much of Mesozoic time and that demonstrate the forearc and retroarc basins sampled different parts of the arc and therefore may record different magmatic histories. In addition, we identified a minor group of Jurassic detrital zircon grains with oceanic geochemical signatures that may have provenance in the Coast Range ophiolite and/or ophiolitic rocks of the western Sierra Nevada metamorphic belt. Taken together, these results suggest that the forearc detrital zircon data set reveals information different from the record within the arc itself, which can help to identify different parts of a continental arc system. Our results highlight the importance of integrating multiple proxies to fully document arc magmatism, and they demonstrate that detrital zircon geochemical data can enhance understanding of a well-characterized arc.

FOREARC DETRITAL ZIRCON AS AVERAGED ARC PROXY

Because zircon is highly refractory and very common in silicic igneous rocks, which dominate continental arc magmatic flare-ups, the detrital zircon record of forearc systems permits broad assessment of magmatic

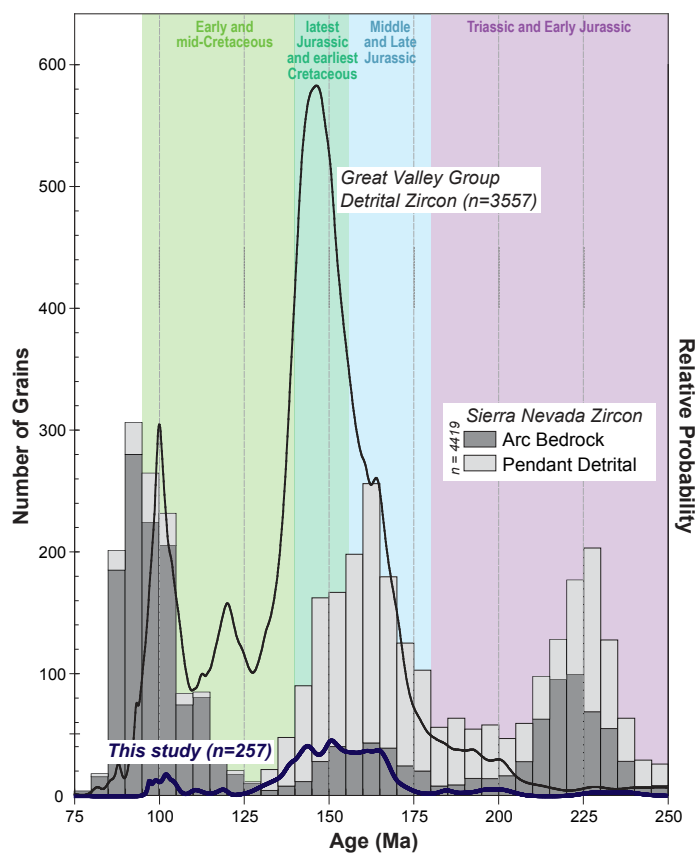


Figure 1. Detrital zircon record from the Great Valley Group ($n = 3557$, shown as probability density function) and zircon record from the Sierra Nevada ($n = 4419$). Sierra Nevada zircon data are shown as histogram of arc bedrock zircon (dark gray) and detrital zircon from metamorphic pendants within the arc (light gray), such that the height of each bin equals the sum of arc bedrock zircon and intra-arc detrital zircon (histogram modified from Paterson and Ducea, 2015). Sierra Nevada data are from Paterson and Ducea (2015). Great Valley Group data are from DeGraaff-Surpless et al. (2002), Surpless et al. (2006), Wright and Wyld (2007), Surpless and Augsburger (2009), Surpless (2014), Sharman et al. (2015), Martin and Clemens-Knott (2015), and Greene and Surpless (2017). Probability density function of detrital zircon ages used in this study ($n = 257$) is shown as thick black line. Background colors indicate four age bins used in this study.

arc activity through time (e.g., de Silva et al., 2015). Although detrital zircon cannot serve as a proxy for isolated parts of a magmatic arc, the detrital zircon record represents a long-term, integrated average record of arc magmatism (e.g., Barth et al., 2013; de Silva et al., 2015) and thus provides a valuable complement to studies of magmatic rocks (e.g., Ducea et al., 2015). Because dated detrital zircon grains can provide a proxy of averaged erosion rates of both upper-crustal arc segments and ancient, eroded arc segments, detrital zircon age populations can be used to assess arc duration, pulses and lulls in magmatic activity (e.g., Barth et al., 2013), and possibly magma addition rates (e.g., Ducea et al., 2015; Paterson and Ducea, 2015). In this study, we extend the utility of detrital zircon beyond U-Pb ages to consider trace-element concentrations as additional proxies with which to better understand Sierran magmatic arc conditions through time.

Numerous studies have linked the Great Valley forearc to the Sierran magmatic arc using sandstone composition and petrofacies (e.g., Ojagan-gas, 1968; Dickinson and Rich, 1972; Mansfield, 1979; Ingersoll, 1983;

Short and Ingersoll, 1990), conglomerate clast compositions (e.g., Rose and Colburn, 1963; Bertucci, 1983; Seiders, 1983), detrital zircon age distributions (e.g., DeGraaff-Surpless et al., 2002; Surpless et al., 2006; Cassel et al., 2012; Martin and Clemens-Knott, 2015; Sharman et al., 2015), isotopic analysis (Linn et al., 1991), geochemical analysis (e.g., van de Kamp and Leake, 1985; Surpless, 2014), paleocurrent analysis (e.g., Ojakangas, 1968; Ingersoll, 1979; Suchecki, 1984), paleobathymetry (e.g., Ingersoll, 1979; Haggart, 1986; Williams, 1997), and seismic stratigraphy and stratigraphic architecture (e.g., Moxon, 1990; Williams, 1997; Constenius et al., 2000; Mitchell et al., 2010; Williams and Graham, 2013). Wright and Wyld (2007) proposed an alternative model that places the basal Great Valley strata (Stony Creek Formation) south of the Sierra Nevada, with postulated northward translation complete by ca. 120 Ma.

The Sacramento and San Joaquin Basins form the northern and southern subbasins of the Great Valley forearc basin, respectively, and are separated by the Cenozoic Stockton arch. Great Valley Group strata in the Sacramento Valley outcrop belt were deposited in more distal environments than strata in the San Joaquin Valley outcrop belt, with basin plain, outer fan, midfan, and slope environments typical of the Sacramento Valley, and midfan, inner fan, and slope environments typical of the San Joaquin Valley (Ingersoll, 1979). These differences resulted from the more eastern location of San Joaquin Valley outcrops, which were closer to inferred paleoshorelines, resulting in more proximal deposits (Ingersoll, 1979).

SAMPLES AND METHODS

We selected seven previously dated detrital zircon samples from throughout the Great Valley Group to broadly capture magmatic arc conditions through time and space. The seven samples span the length of the Great Valley forearc, with three samples from the northern Sacramento Valley (Stony Creek Formation and Ten Mile Member of the Chico Formation), one sample from the southern Sacramento Valley outcrop belt (Venado Formation), and three samples from the northern (Panoche Formation) and southern (Gravelly Flat Formation) San Joaquin outcrop belt (Fig. 2A). These seven samples also encompass the depositional age range of Great Valley Group strata, with two Stony Creek Formation samples collected from the basal Great Valley Group (Tithonian[?] to Berriasian age), two Gravelly Flat Formation samples, the Panoche Formation sample, and the Venado Formation sample collected from Albian to Cenomanian strata spanning the middle of Great Valley Group sedimentation, and the Chico Formation sample collected from Campanian strata in the upper Great Valley Group (Fig. 2B). These seven samples also include a range of sandstone compositions and contain a wide range in the relative abundance of volcanic and metamorphic lithic grain types (Fig. 3; Data Repository Table DR1¹). Because detrital zircon grains were separated from sandstone samples with volcanogenic (24% of analyzed zircon grains), arkosic (44% of grains), and mixed compositions (32% of analyzed zircon grains), these detrital zircons likely provide a geochemical record of both volcanic and plutonic arc magmatism.

Trace-element concentrations in the selected detrital zircon grains (Data Repository Table DR2) were measured by sensitive high-resolution ion microprobe–reverse geometry (SHRIMP-RG), following Mazdab and Wooden (2006). We used cathodoluminescence or backscattered electron images to guide analysis of previously dated grains, placing trace-element pits as close to filled U–Pb pits as the clastic grain morphology permitted. We verified prior age determinations with low-precision U–Pb ages collected simultaneously with trace-element data and calibrated to the R33

standard zircon. Trace-element concentrations were standardized against Madagascar green (MAD) zircon (Barth and Wooden, 2010). Additional trace-element concentrations of zircon from Early Cretaceous plutons of the southern Sierra Nevada and latest Jurassic to earliest Cretaceous zircon of the Kern Plateau were measured via SIMS on a CAMECA IMS 1270 using an oxygen primary ion source with 20 μ A beam intensity, following Montealeone et al. (2007; see Data Repository Table DR3). Low mass resolving power was used to measure trace-element peaks and accompanying REE oxide interferences; REE/REE-oxide ratios were characterized using doped glasses, and trace-element concentrations were calculated by peak-stripping and calibrated to 91500 standard zircon. In order to directly compare SHRIMP-RG and CAMECA data, we calculated a simple conversion factor for CAMECA data by calibrating CAMECA 91500 values to SHRIMP-RG 91500 values that were standardized to MAD zircon.

RESULTS

All Great Valley Group detrital zircon plot within the field of continental zircon defined by Grimes et al. (2007) for U/Yb and Hf (ppm), although several grains plot on or close to the upper limit of U/Yb defined for unambiguously oceanic zircon (Fig. 4). Additional proxies of Sc/Yb and Nd/Yb, used to distinguish continental-arc, ocean-island, and oceanic zircon, provide greater confidence in provenance discrimination, given the range in values and potential for overlap (Grimes et al., 2015). On these discrimination diagrams, most Great Valley Group detrital zircon grains plot within the continental arc field, but 11 grains plot in the oceanic zircon field, and seven grains plot with the ocean-island–type zircon (Fig. 5). We therefore excluded these 18 detrital grains in our comparisons of Great Valley Group detrital zircon trace-element geochemistry with Sierran arc zircon geochemistry.

To ensure that the remaining 239 detrital zircon grains from our seven samples fully represent magmatic activity in the arc through time, we searched for potential differences in zircon geochemistry based on sample location, depositional age, and composition. Samples from the Sacramento and San Joaquin subbasins show near-complete overlap in bivariate plots of selected geochemical ratios (Fig. 6A), suggesting that detrital zircon deposited in the northern basin are not geochemically distinct from detrital zircon in the southern basin. Similarly, geochemical overlap in detrital zircon from samples of different depositional age (Fig. 6B) and from samples of different sandstone compositions (Fig. 6C) indicates that the detrital zircon geochemical signature represents an effective average of arc conditions through time. Significantly, the two Stony Creek samples from the basal Great Valley Group (depositional age of ca. 145 Ma) and the other five Great Valley Group samples (depositional ages of ca. 100 Ma and 80 Ma) show complete overlap of detrital zircon geochemical signatures (Fig. 6B), consistent with provenance in the Sierran arc throughout deposition of the Great Valley Group. These results do not support the translational Great Valley Group model of Wright and Wyld (2007).

To document overall changes in the Sierran arc through Mesozoic time, we divided the Great Valley Group detrital zircon data into four age bins based on their crystallization ages (Fig. 1). These age bins were guided by the detrital zircon age distribution, but they also account for key pulses in the magmatic arc. The Triassic and Early Jurassic (250–180 Ma) bin corresponds in age to the Triassic magmatic pulse and Early Jurassic lull (Barth et al., 2013); the Middle to Late Jurassic (180–156 Ma) bin encompasses the peak of the Middle-to-Late Jurassic pulse implied by Sierra Nevada zircon (Paterson and Ducea, 2015), as well as ages of ophiolites

¹GSA Data Repository Item 2019264, sandstone compositional data, zircon trace element data, supplementary data plots, is available at <http://www.geosociety.org/datarepository/2019>, or on request from editing@geosociety.org.

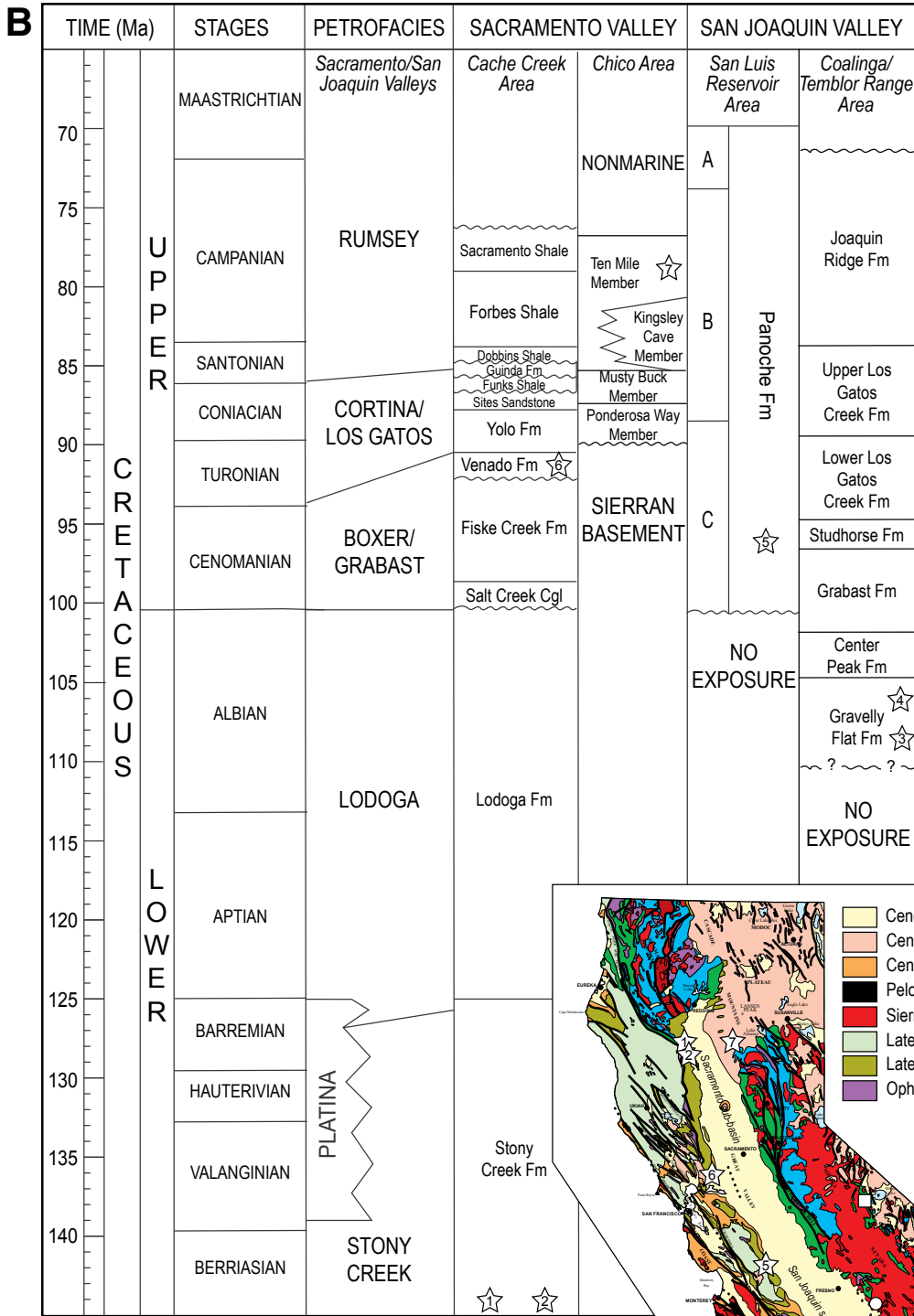
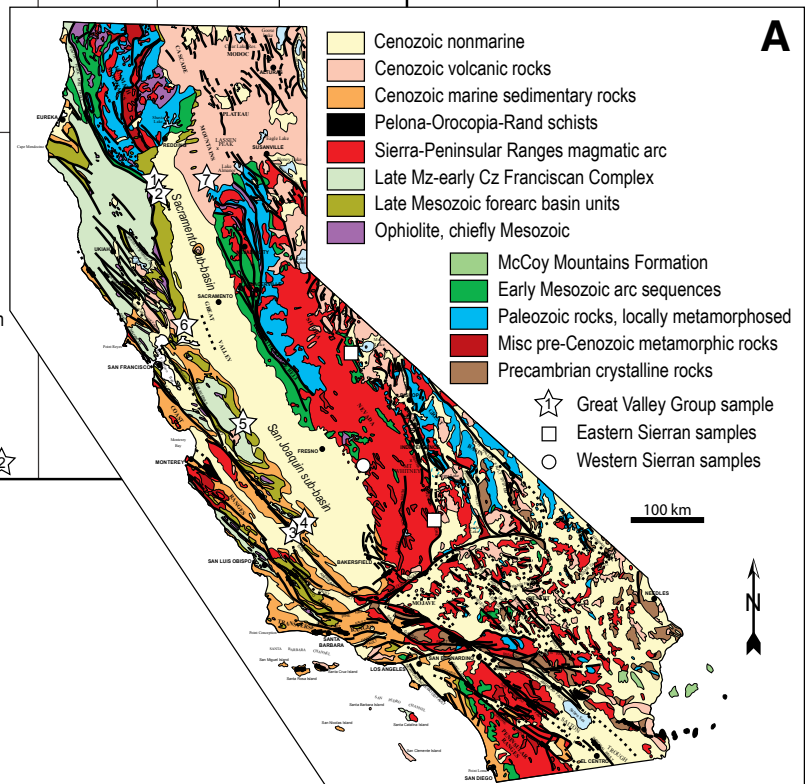


Figure 2. (A) Geologic map of California showing the locations of the seven Great Valley Group (GVG) samples (white stars with numbers), as well as eastern Sierran arc samples (white squares) from the eastern high Sierra (north) and Kern Plateau (south) regions, and western Sierran arc samples (white circle) from the Stokes Mountain region. Map is modified from California Geological Survey (2010). Mz—Mesozoic; Cz—Cenozoic; Misc—miscellaneous. (B) Schematic stratigraphy and petrofacies of the Great Valley Group showing seven sample locations (white stars with numbers). Wavy lines indicate unconformities in each section; petrofacies are from Ingersoll (1979, 1983); Cache Creek section stratigraphy is from Williams and Graham (2013); Chico stratigraphy is from Russel et al. (1986); San Luis Reservoir stratigraphy is from Schilling (1962) and Moxon (1990); and Coalinga/Tembler Range stratigraphy is from Mansfield (1979). Fm—Formation; Cgl—Conglomerate.



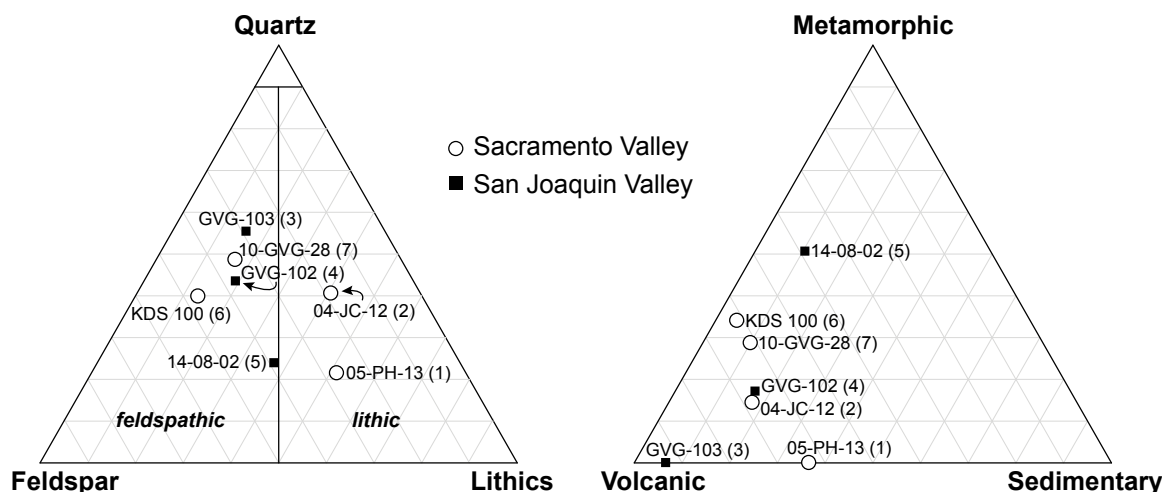


Figure 3. Ternary diagrams showing sample compositions and relative abundance of different lithic types for samples collected from the Sacramento Valley (open circles) and San Joaquin Valley (filled squares). Numbers in parentheses correspond to sample numbers given in location map and stratigraphy in Figure 2.

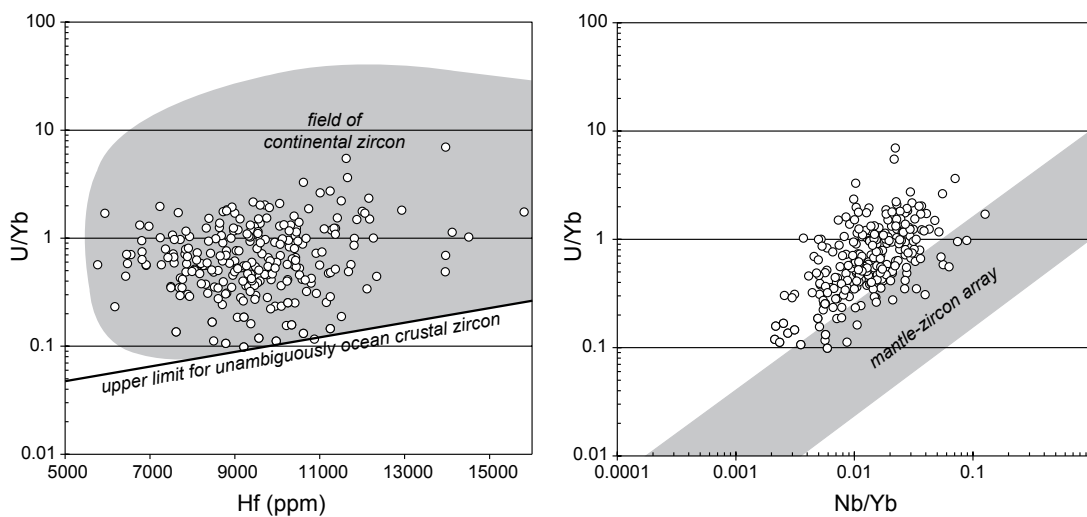


Figure 4. All Great Valley Group detrital zircon data (white circles) plotted on discrimination fields of Grimes et al. (2007).

in the Klamath–Sierran–Coast Ranges region; the latest Jurassic to earliest Cretaceous (156–140 Ma) bin postdates ophiolite formation and centers on the Late Jurassic peak recorded by Great Valley Group detrital zircon; and the Early to mid-Cretaceous (140–95 Ma) bin includes the Early Cretaceous arc and much of the mid-Cretaceous magmatic pulse.

COMPARATIVE ZIRCON TRACE-ELEMENT GEOCHEMISTRY

Sierran Arc

Arc zircon geochemistry is primarily controlled by the extent of melt fractionation during zircon growth and magma source variations that result in variable melt compositions at zircon saturation (Walker et al.,

2010; Claiborne et al., 2010; Barth et al., 2013; Coombs and Vazquez, 2014). Arc zircons are characterized by enrichment in U and Th, reflecting the slab contribution to arc magmas, and depletion in Nb and heavy rare earth elements (HREEs), which are conserved in the slab (Barth et al., 2017; Schmitt et al., 2018). Hf concentration serves as a proxy for the extent of magma fractionation; Hf is typically inversely correlated with Ti, reflecting evolving melt composition with decreasing temperature, and positively correlated with increasing Th, U, and REEs (Barth et al., 2013). Using Yb as representative of HREEs, Grimes et al. (2015) hypothesized that arc zircon would show enrichment in Sc/Yb due to elevated water content and lack of extensive basalt fractionation in arc parent melts prior to zircon saturation, i.e., with increasing U/Yb, Sc/Yb tends to decrease. Arc suites may be differentiated based on U/Yb enrichment,

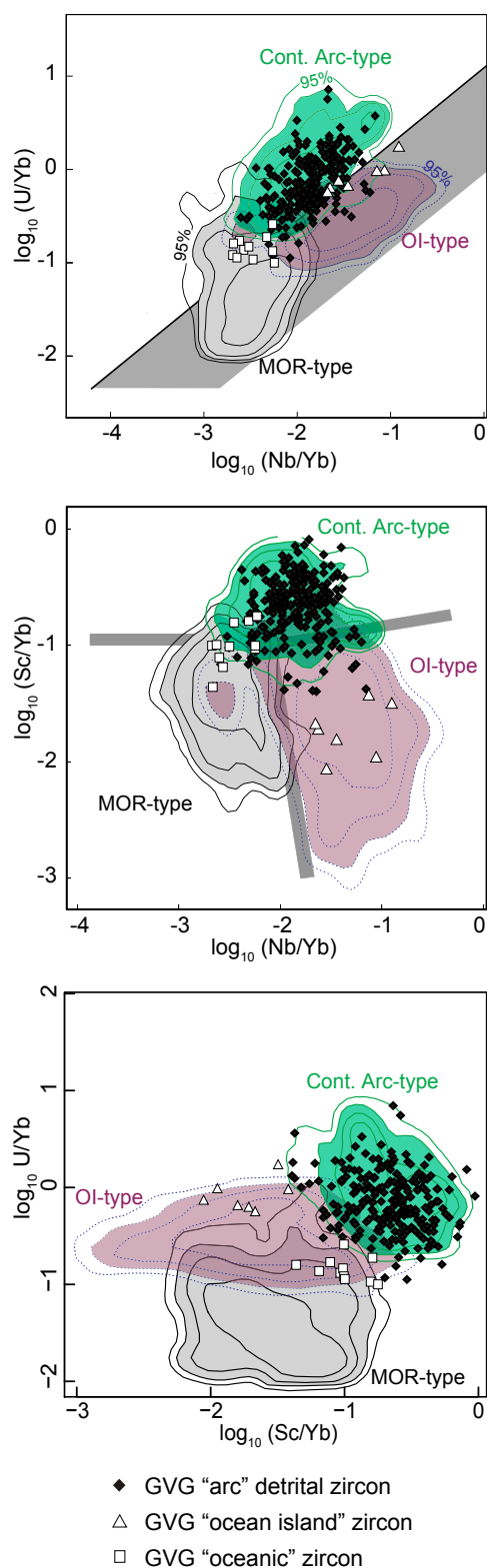


Figure 5. All Great Valley Group detrital zircon data (GVG; diamonds, squares, and triangles) plotted on discrimination fields of Grimes et al. (2015). Black diamonds are considered “continental arc-type” zircon, white squares indicate possible “oceanic” zircon (“mid-ocean-ridge [MOR] type”), and white triangles indicate possible “ocean-island” (“OI-type”) zircon.

with ocean arcs showing the lowest U/Yb values and potassic continental arcs having the highest values (Barth et al., 2017; Schmitt et al., 2018). Ce/Yb and Gd/Yb provide measures of light and middle REE enrichment, respectively, relative to HREE, and they can help to monitor fractional crystallization processes that influence trace-element concentrations in zircon (Grimes et al., 2015). Zircons show large ranges in trace-element abundances within suites and even within single grains, but they also record systematic variation in the ratios of trace elements (Grimes et al., 2007, 2015; Barth et al., 2013). Following Grimes et al. (2007, 2015) and Barth et al. (2013, 2018), we used U/Yb, Nd/Yb, and Sc/Yb to distinguish continental arc-type zircon, and U/Yb, Ce/Yb, Gd/Yb, Th/U, and Hf concentrations to document trends in zircon trace-element geochemistry and highlight differences in zircon populations.

Zircon trace-element data from in situ volcanic and plutonic rocks of the eastern Sierra Nevada include Triassic and Jurassic ignimbrites sampled from intrabatholithic pendants in the eastern high Sierra and coeval granodioritic to granitic components of the underlying batholith (Barth et al., 2012, 2018), as well as latest Jurassic to earliest Cretaceous granite and gabbro from the Kern Plateau. Zircon trace-element data from the western Sierra Nevada include Early Cretaceous gabbro and granitoid samples from the western Stokes Mountain region. We acknowledge that these published and new zircon trace-element data from Sierran volcanic and plutonic rocks provide only a limited record of arc magmatism, but they serve here as a basis for comparison with the detrital zircon record preserved in forearc and retroarc systems. A wider sampling of the arc and forearc to develop a more comprehensive zircon trace-element data set will permit further testing of ideas we present here.

Middle and Late Jurassic zircon (180–156 Ma age group) are generally distinct from older (Triassic and Early Jurassic, 250–180 Ma) and younger (latest Jurassic to Cretaceous zircon, 156–140 Ma and 140–95 Ma) groups and are slightly more diverse in character than Triassic and Early Jurassic zircon (250–180 Ma group; Fig. 7; Data Repository Fig. DR1). The range of Hf concentrations in Sierran zircon remained relatively consistent throughout Mesozoic magmatism (Fig. 7C), suggesting minimal differences in the extent of fractionation across the four age groups; thus, the compositional differences documented here occurred in comparably fractionated intermediate to silicic melts. Based on zircon trace-element geochemistry of eastern Sierran ignimbrites and associated plutonic rocks, Barth et al. (2018) concluded that either silicic magma sources and/or fractionation processes changed systematically from Triassic and Early Jurassic time to Middle and Late Jurassic time in the eastern Sierra. These changes resulted in relatively high U/Yb values in Triassic and Early Jurassic zircon (250–180 Ma), lower U/Yb values in Middle and Late Jurassic (180–156 Ma) zircon, a return to higher U/Yb values in latest Jurassic to earliest Cretaceous (156–140 Ma) zircon, and significantly higher U/Yb values in Cretaceous (140–95 Ma) zircon from the western Sierra (Fig. 7A). Triassic and Early Jurassic (250–180 Ma) zircon grains have distinctly lower Ce/Yb and Th/U values than Middle and Late Jurassic (180–156 Ma) zircon (Figs. 7A–7B). Ce/Yb and Th/U values remained high in latest Jurassic to earliest Cretaceous (156–140 Ma) zircon from the eastern Sierra, but these proxies record lower values in Cretaceous (140–95 Ma) zircon from the western Sierra. Marginally higher Gd/Yb values were found in Middle Jurassic to earliest Cretaceous zircon (180–156 Ma and 156–140 Ma) than in Triassic and Early Jurassic or Cretaceous zircon (250–180 Ma and 140–95 Ma; Fig. 7B).

Great Valley Group

Overall, the 239 Great Valley Group continental-arc detrital zircon grains display remarkably similar values and variability in Th/U and Hf

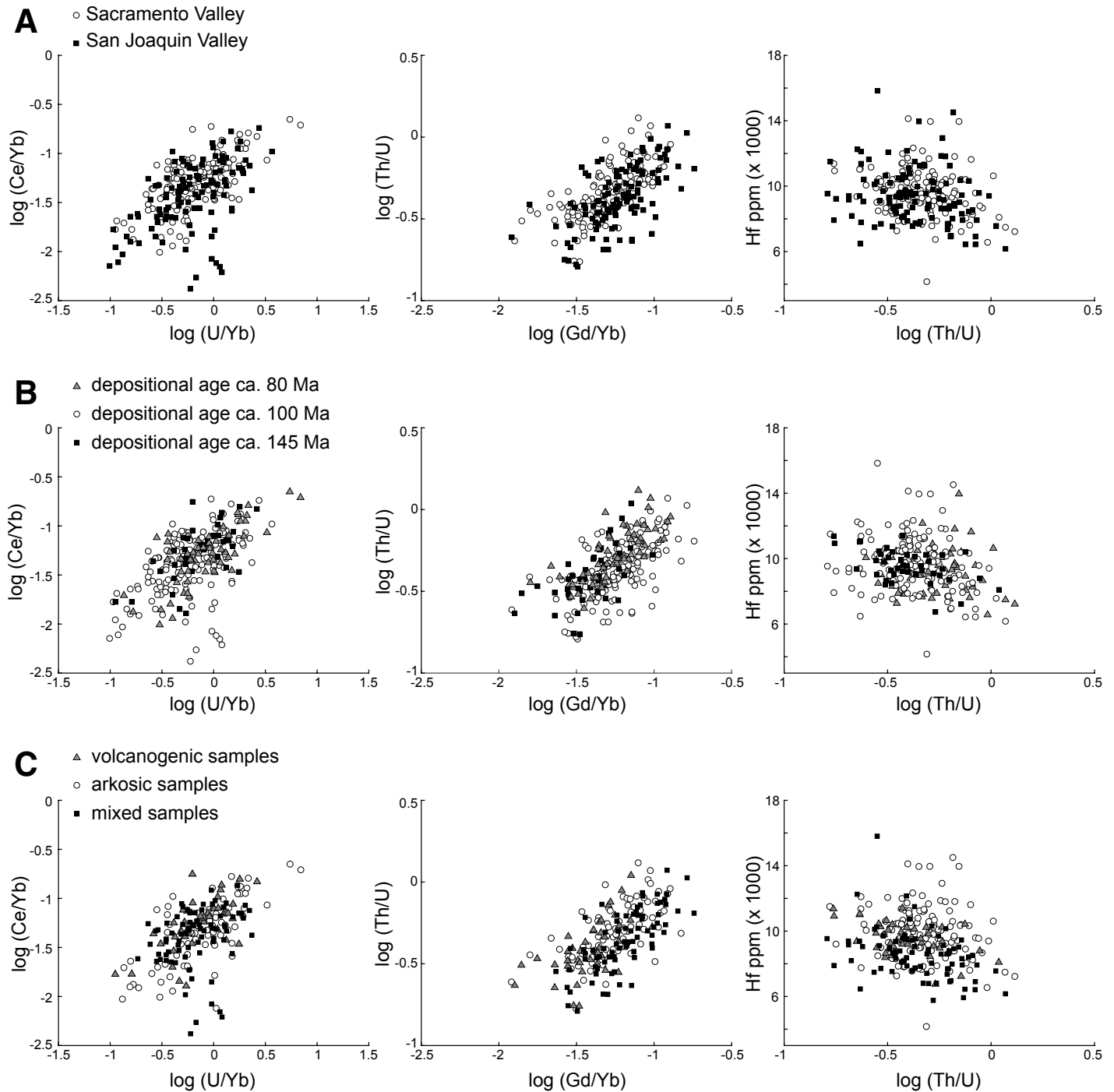


Figure 6. Comparison of Great Valley Group detrital zircon trace-element geochemistry for samples grouped by (A) location in the forearc basin; (B) depositional age; and (C) sandstone composition.

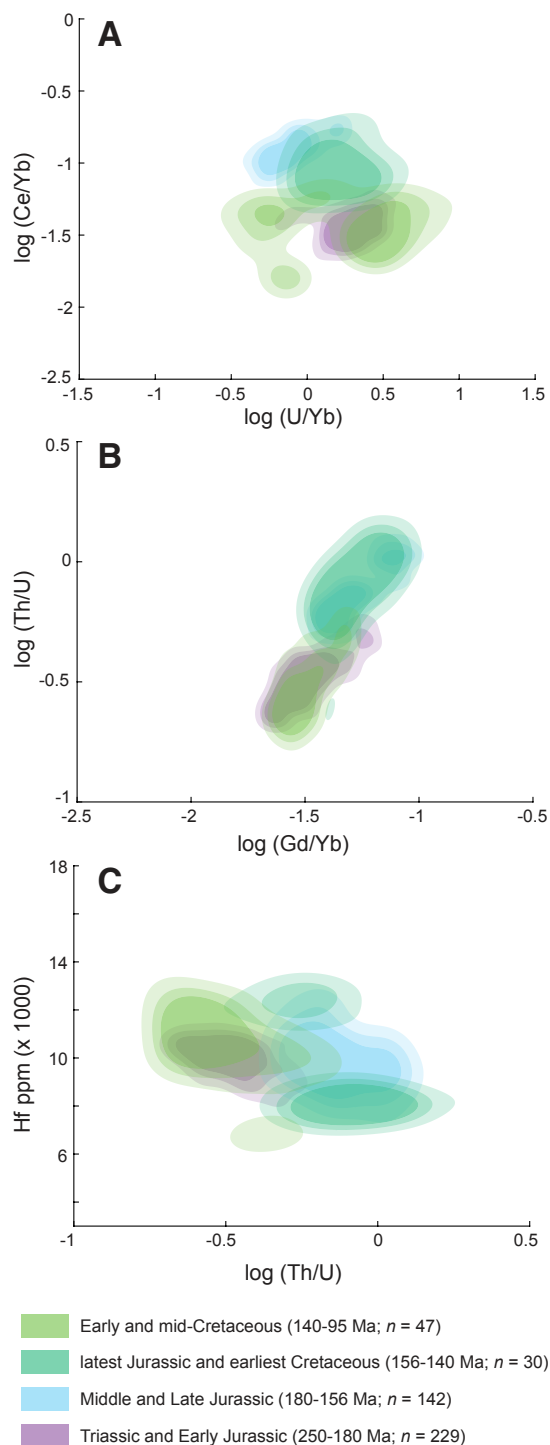


Figure 7. Density distribution plots of geochemical ratios (expressed in \log_{10}) in Sierran zircon for all ages. Colors represent age bins shown in Figure 1; shaded fields are 80%, 65%, and 50% contours of a three-dimensional kernel density distribution surface calculated from the data points, and they represent the proportion of data points that plot within the shading. Density plots were created with MATLAB using the `kde2d` function (a two-dimensional, bivariate kernel density estimator with diagonal bandwidth matrix, evaluated on a square grid; Botev et al., 2010). (A) Plot of $\log(\text{U/Yb})$ vs. $\log(\text{Ce/Yb})$. (B) Plot of $\log(\text{Gd/Yb})$ vs. $\log(\text{Th/U})$; note that the Middle and Late Jurassic zircon plots within the latest Jurassic and earliest Cretaceous field. (C) Plot of $\log(\text{Th/U})$ vs. Hf (ppm) .

concentration across all four age bins (Fig. 8; Data Repository Fig. DR2). Great Valley Group zircon Ce/Yb values were found to be marginally higher in Triassic and Early Jurassic (250–180 Ma) zircon than in younger zircon and showed much greater variability in Middle and Late Jurassic (180–156 Ma) and latest Jurassic and earliest Cretaceous (156–140 Ma) zircon. Middle and Late Jurassic zircon included a distinct subpopulation (10 of 61 grains) of low Ce/Yb and U/Yb zircon (Fig. 8A). Gd/Yb remained relatively consistent through all four age groups of Great Valley Group zircon, with Triassic and Middle Jurassic zircon (250–180 Ma) showing marginally lower values than younger grains, and Middle and Late Jurassic and Cretaceous grains displaying the highest values of Gd/Yb (Fig. 8B). Triassic and Jurassic zircon (250–180 Ma and 180–156 Ma) in the Great Valley Group showed slightly higher U/Yb values than latest Jurassic to Cretaceous (156–140 Ma and 140–95 Ma) zircon (Fig. 8A).

Comparison of Sierran Arc and Great Valley Group Zircon

Comparison of Great Valley Group and Sierran zircon trace-element bivariate plots through the four age bins revealed significant differences between the geochemical signatures of arc zircon and coeval forearc zircon (Fig. 9). Triassic and Early Jurassic zircon (250–180 Ma) displayed the most similarity between arc and forearc zircons, with nearly complete overlap of Th/U, Gd/Yb, and Hf concentration. U/Yb and Ce/Yb ratios showed significant overlap, with marginally higher U/Yb values and lower Ce/Yb values in arc zircon than in forearc zircon.

Middle and Late Jurassic arc and forearc zircon (180–156 Ma) showed similar Gd/Yb and U/Yb values and Hf concentrations, but arc zircons had marginally higher Th/U and distinctly higher Ce/Yb values than forearc zircon (Fig. 9). Ce/Yb and Gd/Yb values, as well as Hf concentrations, remained similar between arc and forearc zircon from latest Jurassic to earliest Cretaceous time (156–140 Ma), but values of U/Yb were distinctly higher in arc than forearc zircon during this period (Fig. 9). Cretaceous zircon (140–95 Ma) from the western arc showed lower Ce/Yb, Gd/Yb, and Th/U values and higher U/Yb values than coeval forearc zircon.

Non-Continental Arc-Type Zircon

On discrimination diagrams of Grimes et al. (2015), 11 Great Valley Group detrital zircon grains plot in the oceanic field, and seven plot with ocean-island zircon (Fig. 5). Typical continental arc grains are characterized by higher U/Yb and Nb/Yb values than oceanic grains and higher Sc/Yb values than ocean-island grains (Grimes et al., 2015). All 11 “oceanic” grains are from only two of the seven samples: Nine “oceanic” grains are from the Gravelly Flat Formation, our southernmost sample in the San Joaquin subbasin, and the other two grains are from the Chico Formation in the northeastern Sacramento subbasin (Fig. 1). Seven Great Valley Group detrital zircon grains plot with the ocean-island-type zircon on discrimination diagrams of Grimes et al. (2015) and in Figure 5 herein. These seven “ocean-island” grains are the focus of continued study to better understand their provenance, and they will not be considered further here.

DISCUSSION

Integrating Arc and Detrital Zircon Data Sets

The geochemical signature of magmatism recorded by forearc detrital zircon was remarkably consistent through time (Fig. 8), even as arc zircon geochemistry varied (Fig. 7) and arc magmatism apparently waxed and waned through magmatic pulses and relative lulls (Fig. 1). In contrast,

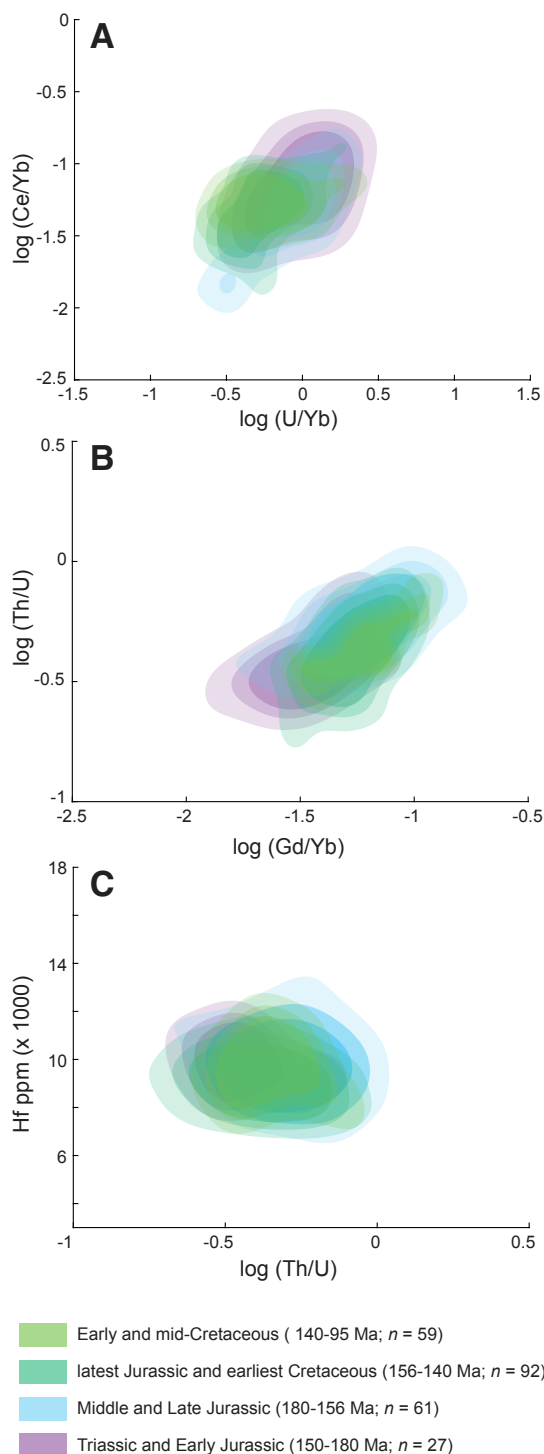


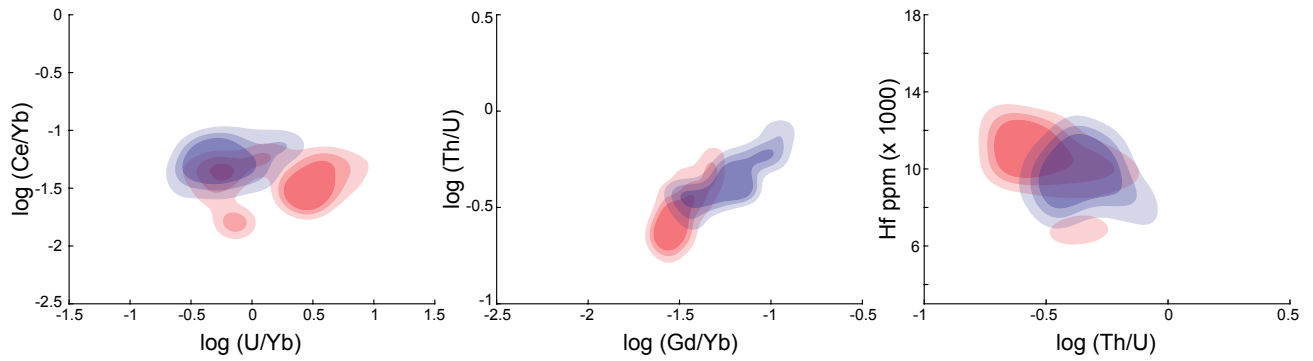
Figure 8. Density distribution plots of key geochemical ratios (expressed in \log_{10}) in Great Valley Group zircon for all ages. Colors represent age bins shown in Figure 1; shaded fields are 80%, 65%, and 50% contours of a three-dimensional kernel density distribution surface calculated from the data points, and they represent the proportion of data points that plot within the shading. Density plots were created with MATLAB using the `kde2d` function (a two-dimensional, bivariate kernel density estimator with diagonal bandwidth matrix, evaluated on a square grid; Botev et al., 2010). (A) Plot of $\log(U/Yb)$ vs. $\log(Ce/Yb)$. (B) Plot of $\log(Gd/Yb)$ vs. $\log(Th/U)$. (C) Plot of $\log(Th/U)$ vs. Hf (ppm).

temporal geochemical changes documented in detrital zircon from the retroarc region (McCoy Mountains Formation; Barth et al., 2013) do track with geochemical variations recorded by Triassic through Jurassic zircon from the eastern Sierran arc (Fig. 10). Differences between arc and retroarc Cretaceous zircon are likely attributable to the western position of most of our Cretaceous arc zircon. The relatively restricted McCoy Mountains Formation may track only the eastern arc, but the much larger forearc basin may contain a spatially averaged, and therefore more consistent, record of arc magmatism. Thus, forearc detrital zircon geochemistry reveals information different from that gleaned from the arc itself. Taken together, these results suggest spatial differences across the arc through time, and they highlight the importance of integrating multiple proxies to fully document arc magmatism.

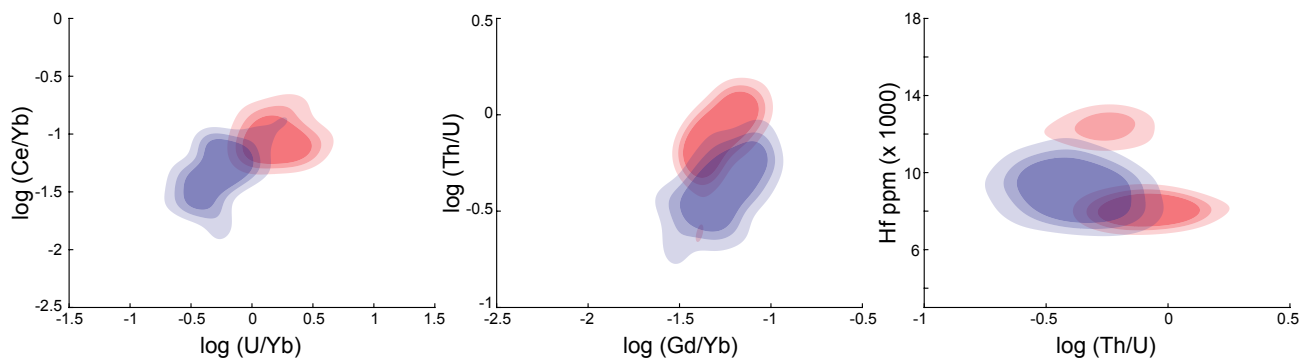
The Great Valley Group and Sierran arc zircon trace-element signatures are most similar in the Triassic and Early Jurassic age group (250–180 Ma), even though all arc zircon within this age group are from the eastern side of the arc; both data sets record similar Hf concentrations and Th/U, although Ce/Yb ranges higher and U/Yb ranges lower in Great Valley Group zircon (Fig. 9). The Triassic and Early Jurassic arc zircon also show the tightest clustering of zircon trace-element compositions across all five parameters, suggesting a compositionally uniform magmatic source. Klemetti et al. (2014) concluded that similarly restricted zircon trace-element compositions, coupled with lower Th concentrations and $\delta^{18}O$ values, measured in Early Jurassic rhyolite in the Mineral King pendant indicated little involvement of continental crust or magmatic precursors. The retroarc data overlap with the Great Valley Group data in all three geochemical plots, including Ce/Yb and U/Yb values, but extend to higher Th/U values (Fig. 10). Greater zircon compositional variability and higher Th/U values in retroarc detrital zircon suggest greater influence of continentally derived melt than indicated by the arc zircon. Thus, differences between arc and detrital zircon geochemistry in early Mesozoic time may largely reflect variability in the involvement of North American cratonal crust and/or enriched lithospheric mantle within a developing continent-fringing magmatic arc (e.g., Barth et al., 2011). These results are consistent with the locus of the initial arc plutonism in a relatively narrow belt extending from the southern Sierra Nevada batholith northwest through the Mojave plateau region (Barth and Wooden, 2006). The similarity in forearc and retroarc zircon geochemistry during this time period suggests that the forearc and retroarc detrital zircon grains form a well-integrated geochemical record of Triassic and Early Jurassic magmatism, which is broadly consistent with zircon results from the eastern Sierran arc.

In contrast to the Triassic and Early Jurassic record, Middle and Late Jurassic (180–156 Ma) magmatism is characterized by two distinct geochemical suites of zircon: Retroarc detrital zircon was derived from a high Ce/Yb and Th/U eastern arc like that characterized by eastern Sierran arc zircon, and forearc detrital zircon was derived from a western arc with lower Ce/Yb and Th/U values (Fig. 10). The eastern Sierran arc zircon and the retroarc detrital zircon overlap in all three bivariate plots for Middle and Late Jurassic zircon (180–156 Ma); in contrast, the Middle and Late Jurassic forearc record reflects greater variability in zircon composition, and it is similar to the Triassic and Early Jurassic forearc record, with the exception of a subpopulation of 10 low Ce/Yb and U/Yb detrital zircon grains (Figs. 8 and 10). Although these 10 grains plot with “continental arc” zircon on discrimination diagrams of Grimes et al. (2015), shown in Figure 5, they share low U/Yb, Ce/Yb, Sc/Yb, and Nb/Yb values with the 11 detrital zircon grains that plot in the “oceanic” field (Figs. 11A and 11B), suggesting that this subpopulation may share ophiolitic sources with the 11 grains interpreted as “oceanic” in origin. Even excluding this Middle Jurassic subpopulation, the remaining “continental arc” detrital zircon data suggest development of clear differences in Middle and Late

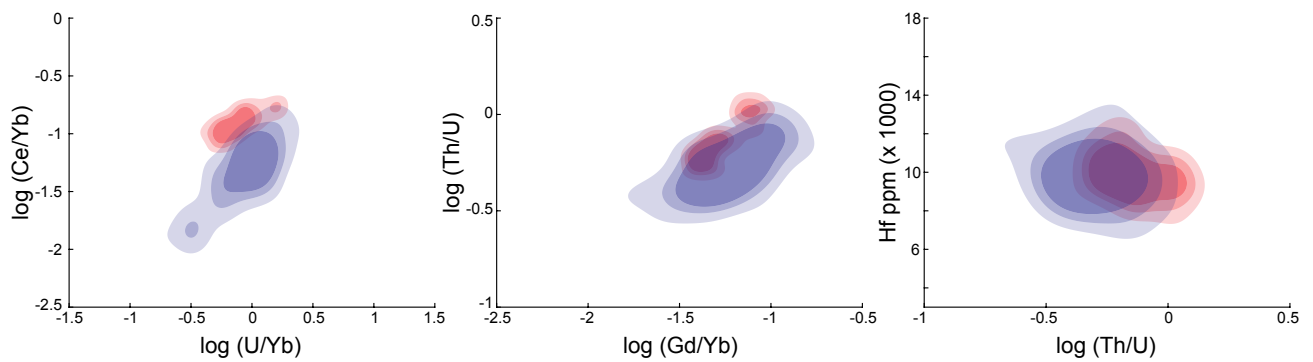
Cretaceous (140-95 Ma)



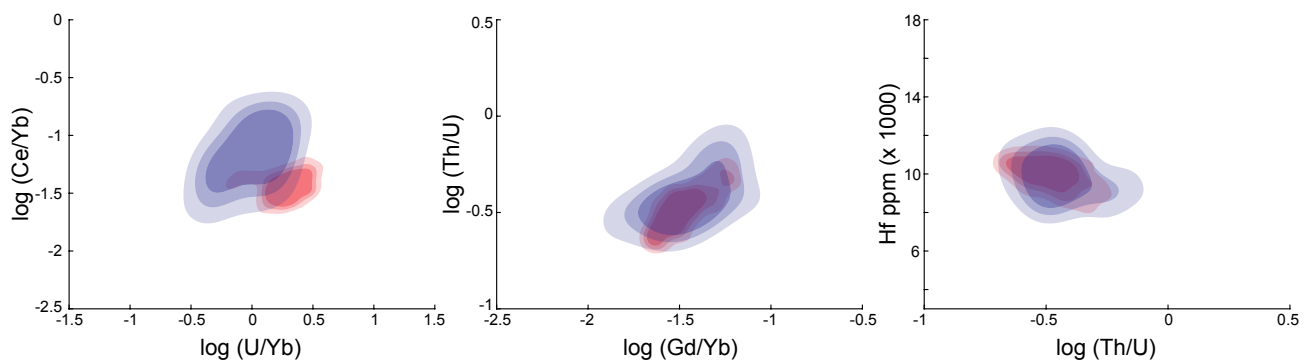
Latest Jurassic and earliest Cretaceous (156-140 Ma)



Middle and Late Jurassic (180-156 Ma)



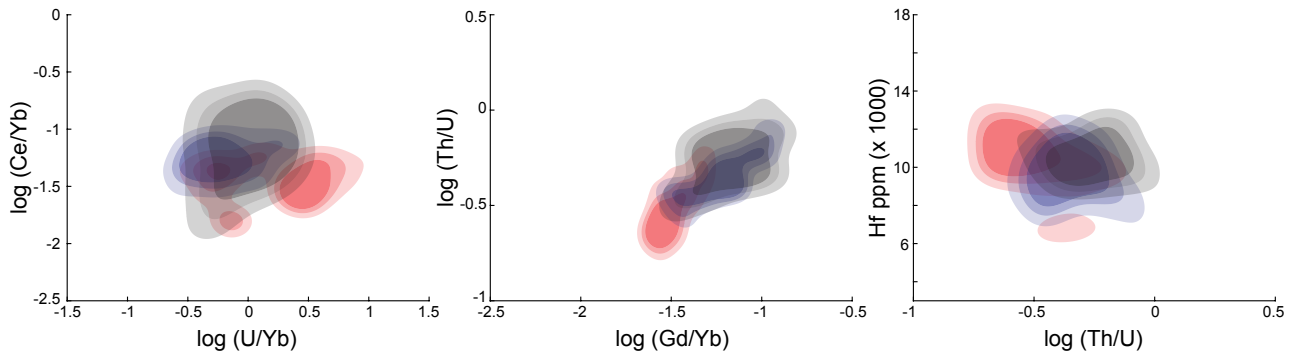
Triassic and Early Jurassic (250-180 Ma)



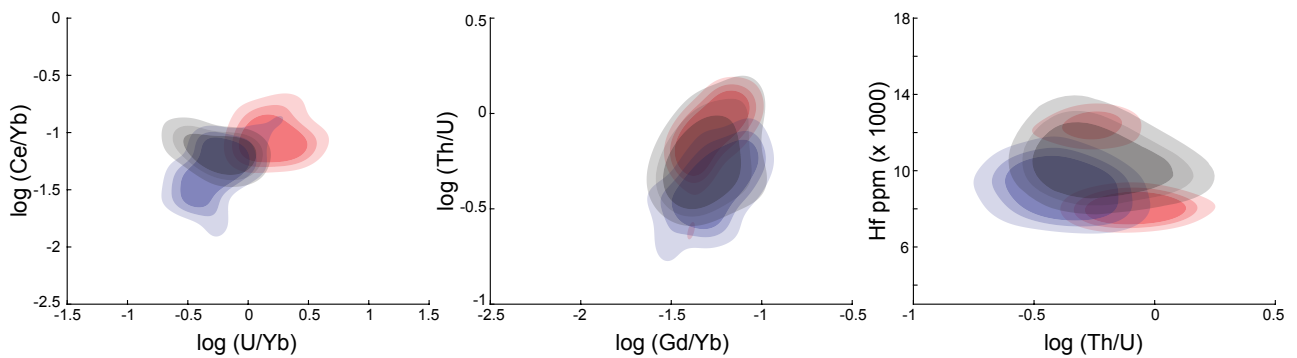
■ Sierran zircon
 ■ GVG detrital zircon

Figure 9. Comparison of Sierran arc (red) and Great Valley Group (GVG; blue) density distributions by age bin. Shading represents 80% (lightest), 65%, and 50% (darkest) of the data that fall within the contours.

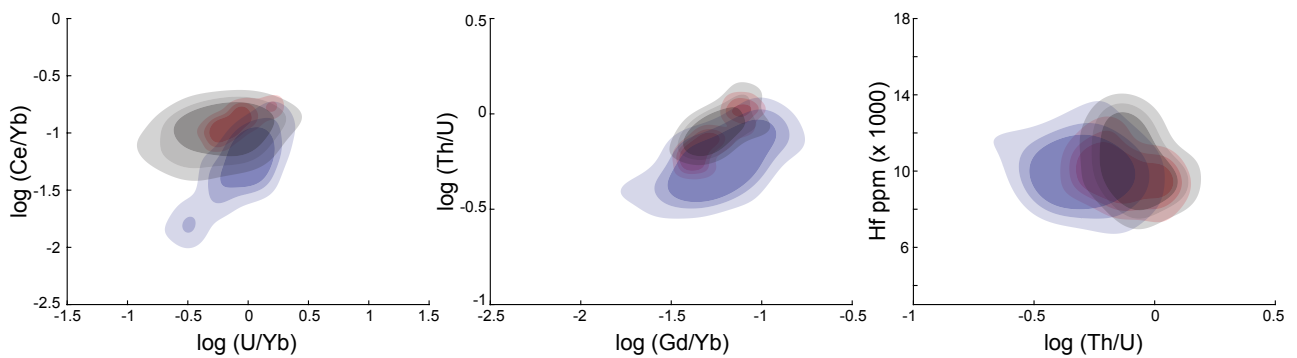
Cretaceous (140-95 Ma)



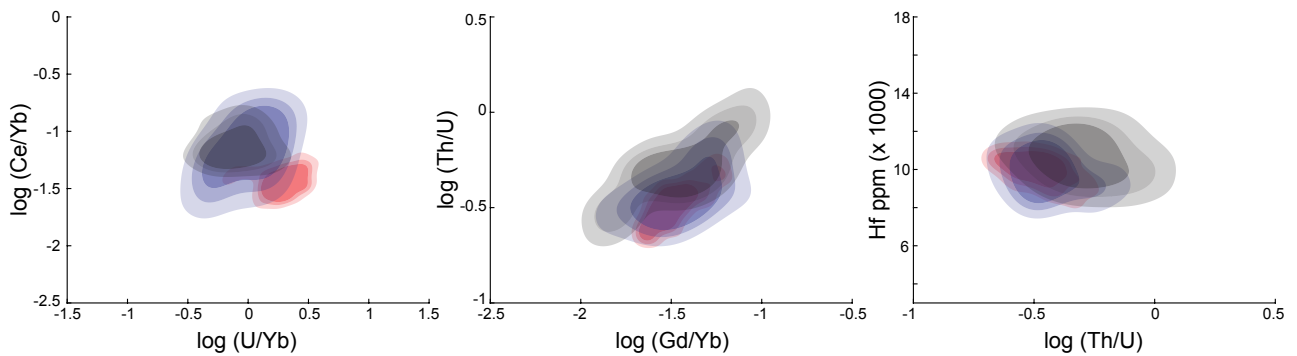
Latest Jurassic and earliest Cretaceous (156-140 Ma)



Middle and Late Jurassic (180-156 Ma)



Triassic and Early Jurassic (250-180 Ma)



Sierran zircon
 GVG detrital zircon
 McCoy Mountains Formation detrital zircon

Figure 10. Comparison of Sierran (red), Great Valley Group (GVG; blue), and McCoy Mountains Formation (gray) density distributions by age bin. Shading represents 80% (lightest), 65%, and 50% (darkest) of the data that fall within the contours.

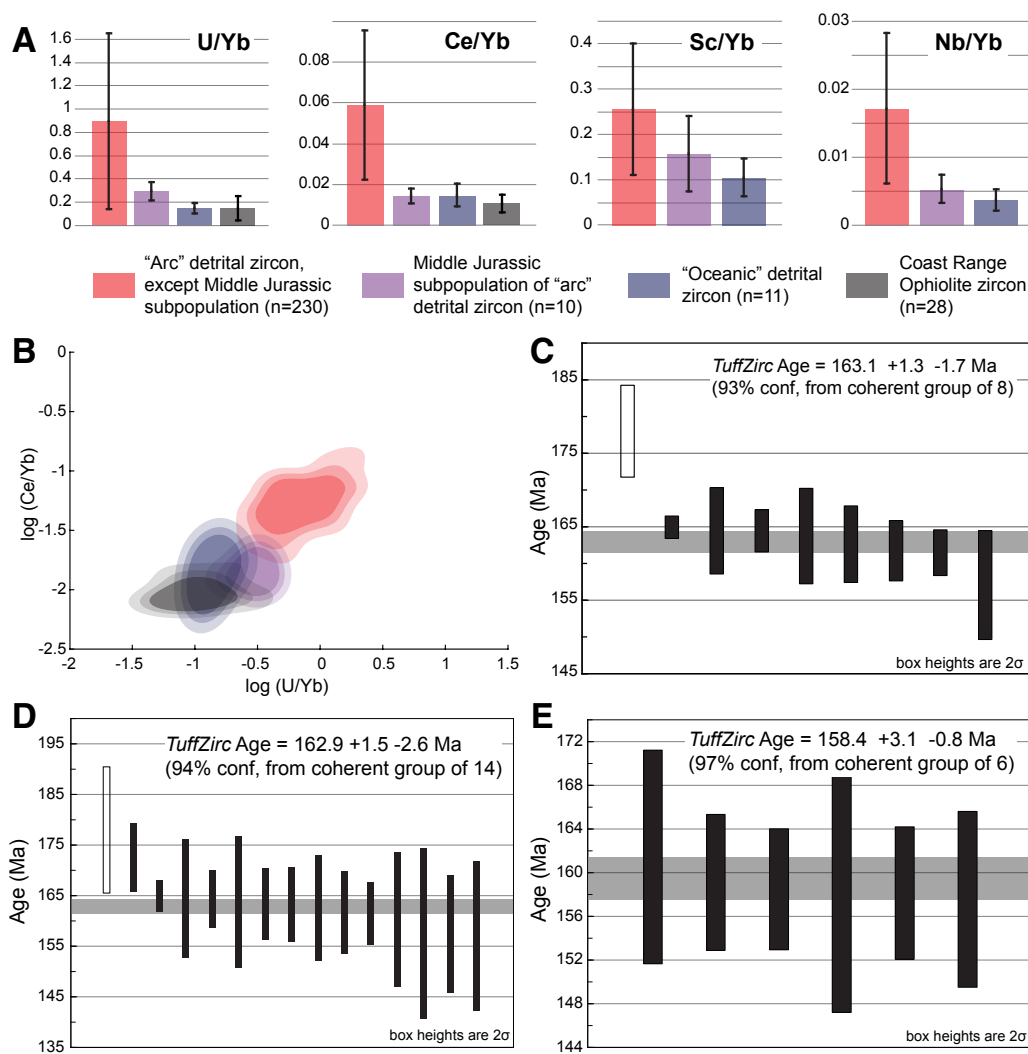


Figure 11. (A) Average values of key geochemical ratios for Great Valley Group (GVG) "arc" detrital zircon (red; excluding 10 grains of the Middle Jurassic subpopulation), the Great Valley Group Middle Jurassic subpopulation of "arc" detrital zircon (purple), the 11 Great Valley Group "oceanic" grains (dark blue), and Coast Range ophiolite zircon (gray) from Colgan and Stanley (2016). (B) Comparison of Great Valley Group detrital zircon "arc," Middle Jurassic subpopulation, and "oceanic" grains with Coast Range ophiolite zircon; shading represents 80% (lightest), 65%, and 50% (darkest) of the data that fall within the contours. (C) Age of "oceanic" zircon from Gravelly Flat Formation samples, San Joaquin subs basin. (D) Age of "oceanic" detrital zircon and Middle Jurassic subpopulation grains from Gravelly Flat Formation. (E) Age of "oceanic" and Middle Jurassic subpopulation grains from Chico Formation. Ages in C, D, and E were calculated using TuffZirc routine in Isoplot 3.6 (Ludwig, 2008).

Jurassic magmatism across the Sierran arc. These differences in arc zircon geochemistry likely resulted from arc magmatism spanning a fundamental lithospheric boundary that resulted in greater involvement in magmatism of continental lithosphere in the eastern arc than in the western arc.

The detrital zircon record may be a more robust indicator of overall arc character than the available arc zircon record for latest Jurassic to earliest Cretaceous time (156–140 Ma), given the much greater proportion of the detrital record than the arc record (Fig. 1); latest Jurassic to earliest Cretaceous zircon grains are abundant in both the forearc (92 of 250 grains; 37%) and retroarc (46 of 167 grains; 28%) data sets, but they are not well represented in the eastern arc data set (29 of 449 grains; 6%). In addition to the forearc detrital record of earliest Cretaceous arc magmatism, 140–130 Ma plutons documented in the northwestern Sierra Foothills (Saleeby et al., 1989; Day and Bickford, 2004), eastern Great Valley subsurface (May and Hewitt, 1948; Saleeby, 2007), and the San Emigdio–Tehachapi Ranges (Chapman et al., 2012) suggest that Middle–Late Jurassic high-flux magmatism continued into Early Cretaceous time. The latest Jurassic to earliest Cretaceous Great Valley Group detrital zircons crystallized from a less-fractionated melt and lack the elevated Ce/Yb values that characterize the eastern arc zircon (Fig. 10). The eastern arc and retroarc zircon grains record higher Th/U and Ce/Yb values than the forearc zircon grains, but the eastern arc zircon grains also have higher

U/Yb values than the retroarc and forearc detrital zircon grains, recording U/Yb values similar to the Triassic eastern arc zircon (Fig. 10). The differences between forearc and retroarc detrital zircon geochemistry that persisted into earliest Cretaceous time likely indicate continued spatial differences across the arc. Elevated U/Yb values in the limited eastern arc data set may not be representative of the full eastern arc.

The abundance of Cretaceous detrital zircon (140–95 Ma) in the forearc chronicles a period of Early Cretaceous arc magmatism (ca. 120 Ma) that is not well represented in the exposed Sierran arc (Fig. 1). Unlike the Triassic through earliest Cretaceous eastern Sierran arc data, our Cretaceous Sierran arc data set comes from the western margin of the exposed arc (Stokes Mountain region; Fig. 2A). These western Sierran arc zircon grains are characterized by lower Th/U and Gd/Yb values and wide ranging, higher U/Yb values as compared to the forearc detrital zircon from the same age group (Fig. 9). Clearly, arc zircon grains from the relatively mafic Stokes Mountain region, which may comprise the southernmost Early Cretaceous arc (Clemens-Knott and Saleeby, 2013), do not fully characterize the western Early Cretaceous arc. Early Cretaceous retroarc data show some overlap with coeval forearc data, but they have the highest Th/U and Ce/Yb values of the three regions for this age group (Fig. 10). These data suggest that spatial differences in the arc persisted through at least mid-Cretaceous time, and that the forearc detrital

zircon characterizes western arc magmatism, whereas retroarc arc detrital zircon characterizes eastern arc magmatism.

The comparison of arc, forearc, and retroarc zircon geochemistry revealed the presence of geochemically distinct arc magmatism in close proximity through much of Jurassic and Cretaceous time (Fig. 10). Forearc and retroarc detrital zircon grains had different provenance beginning in Middle Jurassic time, with retroarc detrital zircon provenance in the eastern Sierran arc, and forearc detrital zircon provenance in the western arc. These differences in zircon geochemistry persisted through mid-Cretaceous time, suggesting the strong influence of an intra-arc lithospheric boundary on arc magmatism (e.g., Kistler and Peterman, 1973; DePaolo, 1981). The Jurassic arc has been characterized as a low-relief, extensional system (e.g., Saleeby and Busby-Spera, 1992; Busby, 2012; Memeti et al., 2010), with Late Jurassic–earliest Cretaceous intra-arc shortening (Dunne and Walker, 1993, 2004; Barth et al., 2017, 2018) possibly resulting in regional topography within the arc. Our zircon data suggest that there was enough breadth and topography within the Middle Jurassic to Early Cretaceous arc to form a drainage divide, similar to that postulated for the Late Cretaceous arc (DeGraaff-Surpless et al., 2002; Sharman et al., 2015), such that the forearc basin received detritus derived from the western arc, while the retroarc basin received eastern arc detritus.

Interpretation of Non-Continental Arc Zircon in the Great Valley Group

Eleven Great Valley Group detrital zircon grains plot in the “oceanic” field on all three discrimination diagrams of Grimes et al. (2015), and therefore they were not considered further in comparisons of forearc and arc zircon (Fig. 5). Nine of these “oceanic” detrital zircon grains were from the Gravelly Flat Formation, our southernmost sample in the San Joaquin subbasin, and eight of these nine grains formed a coherent age of 163 ± 2 Ma (Fig. 11C). The remaining two “oceanic” grains were from the Chico Formation sample, and their ages were found to be 159 ± 3 and 162 ± 5 Ma. All of these detrital zircon ages overlap with ages of ophiolites mapped in the Klamath Mountains (e.g., Josephine ophiolite, ca. 164–162 Ma; Wright and Wyld, 1986; Harper et al., 1994), the northern Coast Ranges (e.g., the 168–161 Ma Elder Creek and Stonyford Coast Range ophiolite remnants; Shervais et al., 2005; Hopson et al., 2008), the western metamorphic belt of the Sierra Nevada (e.g., Smartville complex, ca. 162–155 Ma; Edelman et al., 1989; Edelman and Sharp, 1989; Saleeby et al., 1989; Day and Bickford, 2004), and southern remnants of the Coast Range ophiolite (Del Puerto Coast Range ophiolite remnant, 161 ± 0.4 Ma, and Llanada remnant, 162 ± 0.4 Ma; Hopson et al., 2008).

In addition to these “oceanic” grains, we identified a subpopulation of 10 Middle to Late Jurassic detrital zircon grains in the Great Valley Group that have low U/Yb, Ce/Yb, Sc/Yb, and Nb/Yb values relative to the rest of the Great Valley Group detrital zircon (Figs. 11A–11B). These grains do not consistently plot within the “oceanic” zircon fields of Grimes et al. (2015) due to marginally higher U/Yb values, and therefore we plotted these grains with the “continental arc”–derived Great Valley Group detrital zircon data (Fig. 8). However, a comparison of average values for the four key ratios that discriminate continental-arc, ocean-island, and oceanic-type zircon revealed that these 10 grains form a subpopulation distinct from the continental-arc detrital zircon and very similar to the detrital zircon identified as “oceanic.” Moreover, the 9 “oceanic” detrital zircon grains and the subpopulation of 10 detrital zircon grains identified in the Middle and Late Jurassic age bin are similar to published zircon geochemical values from zircon derived from the Coast Range ophiolite presently exposed in the Piedras Blancas block on sea cliffs north of San Luis Obispo (Colgan and Stanley, 2016; Figs. 11A–11B). As with the

nine “oceanic” grains, these 10 detrital zircon grains were from the Chico Formation sample (4 grains) and the Gravelly Flat Formation samples (6 grains). Moreover, the ages of these grains overlap with the ages of the 11 identified “oceanic” grains. Taken together, 14 of the 15 grains from the Gravelly Flat Formation form a coherent age of 162.9 ± 2.6 Ma (Fig. 11D), and the six detrital zircon grains from the Chico Formation form a coherent age of 158.4 ± 3.1 Ma (Fig. 11E).

Based on their geochemistry and age, we suggest that the Middle and Late Jurassic subpopulation of detrital zircon does not represent continental arc zircon but instead was derived from an intra-oceanic terrane (e.g., island arc, intra-arc ophiolite, or suprasubduction zone ophiolite). The Chico Formation sample was collected in the northeastern Sacramento Valley, proximal to early Mesozoic island-arc terranes in the western metamorphic belt of the Sierra Nevada (Fig. 2A). In particular, the similarity in ages between the six non-continental arc Chico Formation detrital zircon (158.4 ± 3 Ma) and the Smartville Complex rifted oceanic arc (159 ± 3 Ma; Day and Bickford, 2004) is consistent with sources of Chico Formation detrital zircon within the western metamorphic belt of the Sierra Nevada.

Significantly, we did not find any “oceanic” detrital zircon in the western Sacramento Valley subbasin, although those samples would have been most proximal to the Klamath and northern Coast Ranges ophiolites. Instead, the majority of “oceanic” detrital zircon grains (15 of 21, including the Middle Jurassic subpopulation of detrital zircon) come from our southernmost San Joaquin subbasin sample of the Gravelly Flat Formation. Although “oceanic” detrital zircon would have been diluted by much more abundant “continental arc” zircon in the forearc setting, we suggest that the absence of at least a few “oceanic” grains in the western Sacramento Valley samples, combined with their presence in the southern Gravelly Flat sample, indicates that the “oceanic” detrital zircon at Gravelly Flat was derived from a proximal source within the southern Coast Range ophiolite. Two potential proximal ophiolitic sources for Gravelly Flat “oceanic” zircon include the 161 ± 0.4 Ma Del Puerto Coast Range ophiolite remnant (Hopson et al., 2008) and the 162 ± 0.4 Ma Llanada remnant (Hopson et al., 2008), just north and west of Gravelly Flat, respectively.

If the local Del Puerto or Llanada ophiolite remnants were the source of the ca. 163 Ma “oceanic” grains in the Gravelly Flat sample, the Coast Range ophiolite outer ridge must have been uplifted enough by mid-Cretaceous time to shed sediment into the ca. 100 Ma Gravelly Flat Formation. Dumitru et al. (2010) documented a shift from nonaccretionary to accretionary regimes in the Franciscan accretionary complex at ca. 123 Ma, and Wakabayashi (2015) described accelerated accretion and development of imbricate thrust stacks in the accretionary prism that resulted in uplift and exhumation of basement rocks beginning ca. 120 Ma. Rapid accretion and underthrusting in the accretionary prism could have formed enough topography in an outer-arc ridge for potential submarine mass wasting and exposure of basement Coast Range ophiolite by mid-Cretaceous time. Greene and Surpless (2017) proposed a similar mechanism to explain the presence of outsize ophiolitic blocks in the Cenomanian Panoche Formation, north of Gravelly Flat within the San Joaquin subbasin. Additional data are needed to better establish the provenance of the “oceanic” detrital zircon grains in the Great Valley Group, but their presence requires that their ophiolitic source rocks formed at the same time (ca. 164–158 Ma) as the Middle to Late Jurassic magmatism in the eastern Sierran arc.

Implications for Understanding Arc Magmatism and Tectonics

Pulses of magmatism during Triassic, Middle Jurassic, and mid-Cretaceous time are well documented within the Sierra Nevada arc (Fig. 1; e.g., Barth et al., 2013; Paterson and Ducea, 2015). Although the detrital record is broadly consistent with this history of magmatic flux (Barth et

al., 2013), it includes important differences. For example, the Triassic magmatic pulse at ca. 225 ± 12 Ma is well represented in the overall arc record (Fig. 1; Paterson and Ducea, 2015; Saleeby and Dunne, 2015), the eastern Sierran arc (229 of 449 zircon [51%] in this study; Fig. 7), and the retroarc (Barth et al., 2013), but it is nearly absent from the forearc (Fig. 1; 27 of 250 zircon [11%] in this study; Fig. 8). Similarly, the Middle Jurassic pulse (ca. 161 ± 14 Ma; Paterson and Ducea, 2015) is well documented in the arc and retroarc but is relatively diminished in the forearc, while the forearc data extend the duration of this second magmatic pulse well into Early Cretaceous time, with a peak age of ca. 146 Ma (Fig. 1). Moreover, the forearc data document an Early Cretaceous arc (ca. 120 Ma) that is poorly represented in the retroarc (Barth et al., 2013) and arc (Paterson and Ducea, 2015) records. U-Pb age data from the northern Sierra Nevada suggest a longer-lived Cretaceous flare-up event in the northern reaches of the batholith, with abundant Early to mid-Cretaceous zircon (Cecil et al., 2012). U-Pb age data from Sierra Nevada lithologies found in basement cores from the eastern Great Valley Group reveal extensive Early Cretaceous magmatism (140–115 Ma; Saleeby, 2007; Saleeby and Dunne, 2015), which also crops out within and south of the western metamorphic belt (Clemens-Knott and Saleeby, 1999; Irwin and Wooden, 2001, and references therein; Saleeby, 2011; Lackey et al., 2012). Early Cretaceous (ca. 136–134 Ma) rhyolites within the Mineral King pendant in the southern Sierra Nevada suggest that voluminous rhyolitic volcanism occurred during this purported magmatic lull (Klemetti et al., 2014), and coeval basaltic to dacitic volcanic rocks are sandwiched within the ca. 140–135 Ma Goldstein Peak Formation (Clemens-Knott et al., 2013; Martin and Clemens-Knott, 2015). Together with the forearc data, these results are consistent with the proposal that the Early Cretaceous “lull” in Sierran magmatism may be an artifact of preservation and exposure, rather than a true reduction in magmatism to background flux levels (Clemens-Knott and Saleeby, 2013).

Barth et al. (2013) suggested that differences in the history of Sierran magmatic flux captured by the detrital record reflect asymmetric, migratory arc magmatism. Indeed, well-documented Triassic magmatism in the eastern Sierran arc (Barth et al., 2012, 2018) may have formed near the locus of continental magmatism within the arc, such that its preservation in the detrital record is largely limited to the retroarc region. Marginally higher Th/U values in retroarc detrital zircon hint at even greater involvement of continental crust, in contrast to lower Th/U values of Early Jurassic zircon in rhyolite within the Mineral King Pendant, which were interpreted to represent part of an extensive accreted island-arc volcanic system (Klemetti et al., 2014).

Westward migration of magmatism during Jurassic through Early Cretaceous time could have led to the differences in the abundance of Middle Jurassic through earliest Cretaceous zircon across the arc, with arc and retroarc zircon recording the Middle Jurassic magmatic pulse at ca. 161 Ma, while forearc zircon recorded younger, more westerly magmatism that peaked at ca. 146 Ma. However, Middle to Late Jurassic magmatism documented across the full width of the arc (Saleeby and Dunne, 2015) and abundant Middle and Late Jurassic zircon (i.e., 180–156 Ma) in the eastern arc and retroarc with distinctly different geochemistry than the forearc zircon (Fig. 10) suggest a broad swath of magmatism active across the full width of the arc, rather than any systematic westward migration of magmatism during Jurassic time. Alternatively, magmatism may have developed in two separate, adjacent arcs during Early and Middle Jurassic time, with a continental margin arc and fringing island arcs sutured by latest Jurassic time (e.g., Schweickert and Cowan, 1975; Ingersoll, 2000, 2008; Klemetti et al., 2014; Schweickert, 2015).

Our zircon geochemical data cannot distinguish between these tectonic models, but regardless of the exact tectonic reconstruction, the abundance

of Middle and Late Jurassic zircon in the forearc expands the evidence for continued, ongoing magmatism in the Sierran arc(s) during development of the Coast Range ophiolite from as early as 174 Ma (Shervais et al., 2005) to as late as 156 Ma (Hopson et al., 1981). Further expansion of the age and zircon trace-element character of exposed arc basement, coupled with well-characterized detrital zircon suites, holds the potential for a significantly expanded characterization of arc asymmetry and the tectonic evolution of the Triassic and Jurassic Sierra Nevada.

CONCLUSIONS

Great Valley Group forearc detrital zircon geochemistry, combined with retroarc and arc zircon geochemistry, suggests long-lived, geochemically distinct magmatism across the Sierran arc, consistent with either a broad arc spanning the Panthalassan–North American lithospheric suture or possibly two adjacent arcs active during Middle and Late Jurassic time. Forearc detrital zircon geochemistry remained relatively constant through time and distinct from retroarc and eastern arc geochemistry, implying provenance in the western magmatic arc and further indicating the presence of a persistent drainage divide within the Sierra Nevada throughout forearc deposition. The consistency in Great Valley Group detrital zircon geochemistry between basal and younger samples suggests that detrital zircon provenance remained in the western Sierran arc throughout deposition, which does not support a translational forearc model.

Furthermore, Great Valley Group detrital zircon data sets lengthen the duration of the Middle–Late Jurassic magmatic pulse recognized in arc rocks into Early Cretaceous time, and they record significant Early Cretaceous magmatism characteristic of the western arc that is consistent with the existence of an extensive Early Cretaceous arc now largely buried beneath eastern Great Valley Group sediments. Our detrital zircon data also permit recognition of nonarc zircon with “oceanic” geochemistry that may have been derived from ophiolitic terranes in the western Sierran Foothills belt as well as the Coast Range ophiolite, implying the presence of a significant outer arc high by mid-Cretaceous time. These “oceanic” detrital zircon grains form only a minor component of the total detrital zircon data set, and even that low relative abundance likely represents proximal sources; however, the presence of these grains would not be recognized at all on the basis of U-Pb ages alone.

Our results underscore the importance of integrating multiple proxies to fully document arc magmatism. The small arc database we included here clearly does not fully characterize the arc, just as the much larger zircon age database for the arc does not completely characterize the ages of magmatism. However, the detrital zircon results presented here represent an integrated average of the arc through time, and thus changes in forearc zircon geochemistry trends likely reflect changes within the arc that may in turn be related to tectonic processes. Our results suggest that the forearc detrital zircon data set reveals information different from that gleaned from the arc itself, and they demonstrate that detrital zircon geochemistry may help to identify and differentiate different parts of continental arc systems that have pronounced geochemical variation.

ACKNOWLEDGMENTS

Support for this research was provided by the U.S. National Science Foundation through grants EAR-1347985 (Surpless), EAR-1348078 (Clemens-Knott), EAR-1348059 (Barth), OCE-1558830 (Barth), and the Sally Casanova Pre-Doctoral Scholars Program (Gevedon). M. Coble provided timely guidance and support in the sensitive high-resolution ion microprobe–reverse geometry (SHRIMP-RG) laboratory, and R. Economos and the secondary ion mass spectrometry (SIMS) laboratory staff at the University of California–Los Angeles assisted with CAMECA data collection. We thank Kurt Sundell for assistance in plotting geochemical data, and we thank Joe Wooden, Carl Jacobsen, and Nancy Riggs for insightful discussions and suggestions. Field and laboratory support was provided by undergraduate students B. Alexander, H. Casares, J. Estrada, S. Hensel, J. Hernandez, T. Mistretta, B. Rysak, and J. Shukle. This manuscript benefited from thoughtful comments from reviewers Jay Chapman and M. Robinson Cecil.

REFERENCES CITED

- Arculus, R.J., Gill, J.B., Cambray, H., Chen, W., and Stern, R.J., 1995, Geochemical evolution of arc systems in the western Pacific: The ash and turbidite record recovered by drilling, *in* Taylor, B., and Natland, J., eds., *Active Margins and Marginal Basins of the Western Pacific*: American Geophysical Union Geophysical Monograph 88, p. 45–65, <https://doi.org/10.1029/GM088p0045>.
- Barth, A.P., and Wooden, J.L., 2006, Timing of magmatism following initial convergence at a passive margin, southwestern U.S. Cordillera, and ages of lower crustal magma sources: *The Journal of Geology*, v. 114, p. 231–245, <https://doi.org/10.1086/499573>.
- Barth, A.P., and Wooden, J.L., 2010, Coupled elemental and isotopic analyses of polygenetic zircons from granitic rocks by ion microprobe, with implications for melt evolution and the sources of granitic magmas: *Chemical Geology*, v. 277, p. 149–159, <https://doi.org/10.1016/j.chemgeo.2010.07.017>.
- Barth, A.P., Walker, J.D., Wooden, J.L., Riggs, N.R., and Schweickert, R.A., 2011, Birth of the Sierra Nevada magmatic arc: Early Mesozoic plutonism and volcanism in the east-central Sierra Nevada of California: *Geosphere*, v. 7, p. 877–897, <https://doi.org/10.1130/GES00661.1>.
- Barth, A.P., Feilen, A.D.G., Yager, S.L., Douglas, S.R., Wooden, J.L., Riggs, N.R., and Walker, J.D., 2012, Petrogenetic connections between ash-flow tuffs and a granodioritic to granitic intrusive suite in the Sierra Nevada arc, California: *Geosphere*, v. 8, p. 250–264, <https://doi.org/10.1130/GES00737.1>.
- Barth, A.P., Wooden, J.L., Jacobson, C.E., and Economos, R.C., 2013, Detrital zircon as a proxy for tracking the magmatic arc system: The California arc example: *Geology*, v. 41, p. 223–226, <https://doi.org/10.1130/G33619.1>.
- Barth, A.P., Tani, K., Meffre, S., Wooden, J.L., Coble, M.A., Arculus, R.J., Ishizuka, O., and Shukle, J.T., 2017, Generation of silicic melts in the early Izu-Bonin arc recorded by detrital zircons in proximal arc volcanoclastic rocks from the Philippine Sea: *Geochemistry Geophysics Geosystems*, v. 18, p. 3576–3591, <https://doi.org/10.1002/2017GC006948>.
- Barth, A.P., Wooden, J.L., Riggs, N.R., Walker, J.D., Tani, K., Penniston-Dorland, S.C., Jacobsen, C.E., Laughlin, J.A., and Hiramatsu, R., 2018, Marine volcanoclastic record of early arc evolution in the eastern Ritter Range pendant, central Sierra Nevada, California: *Geochemistry Geophysics Geosystems*, v. 19, p. 2543–2559, <https://doi.org/10.1029/2018GC007456>.
- Bateman, P.C., 1992, Plutonism in the Central Part of the Sierra Nevada Batholith, California: U.S. Geological Survey Professional Paper 1483, 186 p.
- Bertucci, P.F., 1983, Petrology and provenance of the Stony Creek Formation, northwestern Sacramento Valley, California, *in* Bertucci, P.F., and Ingersoll, R.V., eds., *Guidebook to the Stony Creek Formation, Great Valley Group, Sacramento Valley, California*: Los Angeles, California, Pacific Section, Society of Economic Paleontology and Mineralogy, p. 1–16.
- Botev, Z.I., Grotowski, J.F., and Kroese, D.P., 2010, Kernel density estimation via diffusion: *Annals of Statistics*, v. 38, no. 5, p. 2916–2957, <https://doi.org/10.1214/10-AOS799>.
- Busby, C.J., 2012, Extensional and transensional continental arc basins: Case studies from the southwestern United States, *in* Busby, C., and Azor, A., eds., *Tectonics of Sedimentary Basins: Recent Advances*: Oxford, UK, Blackwell Publishing, p. 382–404, <https://doi.org/10.1002/9781444347166.ch19>.
- California Geological Survey, 2010, *Geologic Map of California*: California Geological Survey Geologic Data Map 2, scale 1:250,000.
- Cassel, E.J., Grove, M., and Graham, S.A., 2012, Eocene drainage evolution and erosion of the Sierra Nevada batholith across northern California and Nevada: *American Journal of Science*, v. 312, p. 117–144, <https://doi.org/10.2475/02.2012.03>.
- Cecil, M.R., Rotberg, G.L., Ducea, M.N., Saleeby, J.B., and Gehrels, G.E., 2012, Magmatic growth and batholithic root development in the northern Sierra Nevada, California: *Geosphere*, v. 8, p. 592–606, <https://doi.org/10.1130/GES00729.1>.
- Chapman, A.D., Saleeby, J.B., Wood, D.J., Piasecki, A., Kidder, S., Ducea, M.N., and Farley, K.A., 2012, Late Cretaceous gravitational collapse of the southern Sierra Nevada batholith, California: *Geosphere*, v. 8, no. 2, p. 314–341, <https://doi.org/10.1130/GES00740.1>.
- Chapman, A.D., Ernst, W.D., Gottlieb, E., Powerman, V., and Metzger, E.P., 2015, Detrital zircon geochronology of Neoproterozoic–Lower Cambrian passive-margin strata of the White-Inyo Range, east-central California: Implications for the Mojave–Snow Lake fault hypothesis: *Geological Society of America Bulletin*, v. 127, p. 926–944, <https://doi.org/10.1130/B31142.1>.
- Chapman, J.B., Gehrels, G.E., Ducea, M.N., Giesler, N., and Pullen, A., 2016, A new method for estimating parent rock trace element concentrations from zircon: *Chemical Geology*, v. 439, p. 59–70, <https://doi.org/10.1016/j.chemgeo.2016.06.014>.
- Chen, J.H., and Moore, J.G., 1982, Uranium-lead isotopic ages from the Sierra Nevada batholith, California: *Journal of Geophysical Research*, v. 87, p. 4761–4784, <https://doi.org/10.1029/JB087iB06p04761>.
- Chen, J.H., and Tilton, G.R., 1991, Applications of lead and strontium isotopic relationships to the petrogenesis of granitoid rocks, central Sierra Nevada batholith, California: *Geological Society of America Bulletin*, v. 103, p. 439–447, [https://doi.org/10.1130/0016-7606\(1991\)103<0439:AOLASl>2.3.CO;2](https://doi.org/10.1130/0016-7606(1991)103<0439:AOLASl>2.3.CO;2).
- Claiborne, L.L., Miller, C.F., Flanagan, D.M., Clynne, M.A., and Wooden, J.L., 2010, Zircon reveals protracted magma storage and recycling beneath Mount St. Helens: *Geology*, v. 38, no. 11, p. 1011–1014, <https://doi.org/10.1130/G31285.1>.
- Clemens-Knott, D., and Saleeby, J.B., 1999, Impinging ring dike complexes in the Sierra Nevada batholith, California: Roots of the Early Cretaceous volcanic arc: *Geological Society of America Bulletin*, v. 111, no. 4, p. 484–496, [https://doi.org/10.1130/0016-7606\(1999\)111<0484:IRDCIT>2.3.CO;2](https://doi.org/10.1130/0016-7606(1999)111<0484:IRDCIT>2.3.CO;2).
- Clemens-Knott, D., and Saleeby, J.B., 2013, Mesozoic metasedimentary framework and gabbroids of the Early Cretaceous Sierra Nevada batholith, California, *in* Putirka, K., ed., *Geologic Excursions from Fresno, California, and the Central Valley*: Geological Society of America Field Guide 32, p. 79–98, [https://doi.org/10.1130/2013.0032\(05\)](https://doi.org/10.1130/2013.0032(05)).
- Clemens-Knott, D., van der Kolk, D.A., Sturmer, D.M., and Saleeby, J.B., 2013, The Goldstein Peak Formation, central California: Record of a nonmarine intra-arc basin within the Early Cretaceous Sierra Nevada arc: *Geosphere*, v. 9, no. 4, p. 718–735, <https://doi.org/10.1130/GES00886.1>.
- Coleman, D.S., and Glazner, A.F., 1997, The Sierra Crest magmatic event: Rapid formation of juvenile crust during the Late Cretaceous in California: *International Geology Review*, v. 39, p. 768–787, <https://doi.org/10.1080/00206819709465302>.
- Colgan, J.P., and Stanley, R.G., 2016, The Point Sal–Point Piedras Blancas correlation and the problem of slip on the San Gregorio–Hosgri fault, central California Coast Ranges: *Geosphere*, v. 12, no. 3, p. 971–984, <https://doi.org/10.1130/GES01289.1>.
- Constenius, K.N., Johnson, R.A., Dickinson, W.R., and Williams, T.A., 2000, Tectonic evolution of the Jurassic–Cretaceous Great Valley forearc, California: Implications for the Franciscan thrust-wedge hypothesis: *Geological Society of America Bulletin*, v. 112, p. 1703–1723, [https://doi.org/10.1130/0016-7606\(2000\)112<1703:TEOTJC>2.0.CO;2](https://doi.org/10.1130/0016-7606(2000)112<1703:TEOTJC>2.0.CO;2).
- Coombs, M.L., and Vazquez, J.A., 2014, Cogenetic late Pleistocene rhyolite and cumulate diorites from Augustine Volcano revealed by SIMS ²³⁸U–²³⁰Th dating of zircon, and implications for silicic magma generation by extraction from mush: *Geochemistry Geophysics Geosystems*, v. 15, p. 4846–4865, <https://doi.org/10.1002/2014GC005589>.
- Day, H.W., and Bickford, M.E., 2004, Tectonic setting of the Jurassic Smartville and Slate Creek complexes, northern Sierra Nevada, California: *Geological Society of America Bulletin*, v. 116, p. 1515–1528, <https://doi.org/10.1130/B25416.1>.
- DeGraaff-Surpless, K., Graham, S.A., Wooden, J.L., and McWilliams, M.O., 2002, Detrital zircon provenance analysis of the Great Valley Group, California: Evolution of an arc-forearc system: *Geological Society of America Bulletin*, v. 114, p. 1564–1580, [https://doi.org/10.1130/0016-7606\(2002\)114<1564:DZPAOT>2.0.CO;2](https://doi.org/10.1130/0016-7606(2002)114<1564:DZPAOT>2.0.CO;2).
- DePaolo, D.J., 1981, A neodymium and strontium isotopic study of the Mesozoic calc-alkaline granitic batholiths of the Sierra Nevada and Peninsular Ranges, California: *Journal of Geophysical Research*, v. 86, no. B11, p. 10,470–10,488, <https://doi.org/10.1029/JB086iB11p10470>.
- de Silva, S.L., Riggs, N.R., and Barth, A.P., 2015, Quickening the pulse: Fractal tempos in continental arc magmatism: *Elements*, v. 11, p. 113–118, <https://doi.org/10.2113/gselements.11.2.113>.
- Dickinson, W.R., and Rich, E.I., 1972, Petrologic intervals and petrofacies in the Great Valley sequence, Sacramento Valley, California: *Geological Society of America Bulletin*, v. 83, p. 3007–3024, [https://doi.org/10.1130/0016-7606\(1972\)83\[3007:PIAPIT\]2.0.CO;2](https://doi.org/10.1130/0016-7606(1972)83[3007:PIAPIT]2.0.CO;2).
- Dodge, F.C., Millard, H.T., Jr., and Elsheimer, H.N., 1982, Compositional Variations and Abundances of Selected Elements in Granitoid Rocks and Constituent Minerals, Central Sierra Nevada Batholith, California: U.S. Geological Survey Professional Paper 1248, 29 p., <https://doi.org/10.3133/pp1248>.
- Draut, A.E., and Clift, P.D., 2013, Differential preservation in the geologic record of intraoceanic arc sedimentary and tectonic processes: *Earth-Science Reviews*, v. 116, p. 57–84, <https://doi.org/10.1016/j.earscirev.2012.11.003>.
- Ducea, M., 2001, The California arc: Thick granitic batholiths, eclogitic residues, lithospheric-scale thrusting, and magmatic flare-ups: *GSA Today*, v. 11, no. 11, p. 4–10, [https://doi.org/10.1130/1052-5173\(2001\)011<0004:TCATGB>2.0.CO;2](https://doi.org/10.1130/1052-5173(2001)011<0004:TCATGB>2.0.CO;2).
- Ducea, M.N., Paterson, S.R., and DeCelles, P.G., 2015, High-volume magmatic events in subduction systems: *Elements*, v. 11, p. 99–104, <https://doi.org/10.2113/gselements.11.2.99>.
- Dumitru, T.A., Wakabayashi, J., Wright, J.E., and Wooden, J.L., 2010, Early Cretaceous transition from nonaccretionary behavior to strongly accretionary behavior within the Franciscan subduction complex: *Tectonics*, v. 29, TC5001, <https://doi.org/10.1029/2009TC002542>.
- Dunne, G.C., and Walker, J.D., 1993, Age of Jurassic volcanism and tectonism, southern Owens Valley region, east-central California: *Geological Society of America Bulletin*, v. 105, p. 1223–1230, [https://doi.org/10.1130/0016-7606\(1993\)105<1223:AQJVAT>2.3.CO;2](https://doi.org/10.1130/0016-7606(1993)105<1223:AQJVAT>2.3.CO;2).
- Dunne, G.C., and Walker, J.D., 2004, Structure and evolution of the East Sierran thrust system, east-central California: *Tectonics*, v. 23, TC4012, <https://doi.org/10.1029/2002TC001478>.
- Edelman, S.H., and Sharp, W.D., 1989, Terranes, early faults, and pre-Late Jurassic amalgamation of the western Sierra Nevada metamorphic belt, California: *Geological Society of America Bulletin*, v. 101, p. 1420–1433, [https://doi.org/10.1130/0016-7606\(1989\)101<1420:TEFAPL>2.3.CO;2](https://doi.org/10.1130/0016-7606(1989)101<1420:TEFAPL>2.3.CO;2).
- Edelman, S.H., Day, H.W., and Bickford, M.E., 1989, Implications of U–Pb zircon ages for the Smartville and Slate Creek complexes, northern Sierra Nevada, California: *Geology*, v. 17, p. 1032–1035, [https://doi.org/10.1130/0091-7613\(1989\)017<1032:IOUPZA>2.3.CO;2](https://doi.org/10.1130/0091-7613(1989)017<1032:IOUPZA>2.3.CO;2).
- Gill, J.B., Hiscott, R.N., and Vidal, P., 1994, Turbidite geochemistry and evolution of the Izu-Bonin arc and continents: *Lithos*, v. 33, p. 135–168, [https://doi.org/10.1016/0024-4937\(94\)90058-2](https://doi.org/10.1016/0024-4937(94)90058-2).
- Greene, T.J., and Surpless, K.D., 2017, Facies architecture and provenance of a boulder-conglomerate submarine channel system, Panoche Formation, Great Valley Group: A forearc basin response to middle Cretaceous tectonism in the California convergent margin: *Geosphere*, v. 13, no. 3, p. 838–869, <https://doi.org/10.1130/GES01422.1>.
- Grimes, C.B., John, B.E., Kelemen, P.B., Mazdad, F.K., Wooden, J.L., Cheadle, M.J., Hanghøj, K., and Schwartz, J.J., 2007, Trace element chemistry of zircons from oceanic crust: A method for distinguishing detrital zircon provenance: *Geology*, v. 35, p. 643–646, <https://doi.org/10.1130/G23603A.1>.
- Grimes, C.B., Wooden, J.L., Cheadle, M.J., and John, B.E., 2015, “Fingerprinting” tectono-magmatic provenance using trace elements in igneous zircon: *Contributions to Mineralogy and Petrology*, v. 170, p. 46, <https://doi.org/10.1007/s00410-015-1199-3>.
- Haggart, J.W., 1986, Stratigraphy of the Redding Formation of north-central California and its bearing on Late Cretaceous paleogeography, *in* Abbott, P.L., ed., *Cretaceous Stratigraphy, Western North America*: Pacific Section, Society of Economic Paleontologists and Mineralogists Field Trip Guidebook 46, p. 161–178.
- Harper, G.D., Saleeby, J.B., and Heizler, M., 1994, Formation and emplacement of the Josephine ophiolite and the Nevada orogeny in the Klamath Mountains, California–Oregon: U/Pb zircon and ⁴⁰Ar/³⁹Ar geochronology: *Journal of Geophysical Research*, ser. B, Solid Earth and Planets, v. 99, no. B3, p. 4293–4321, <https://doi.org/10.1029/93JB02061>.

- Hopson, C.A., Mattinson, J.M., and Pessagno, E.A., Jr., 1981, Coast Range ophiolite, western California, *in* Ernst, W.G., ed., *The Geotectonic Development of California*, Rubey Volume I: Englewood Cliffs, New Jersey, Prentice-Hall, p. 418–510.
- Hopson, C.A., Mattinson, J.M., Pessagno, E.A., Jr., and Luyendyk, B.P., 2008, California Coast Range ophiolite: Composite Middle and Late Jurassic oceanic lithosphere, *in* Wright, J.E., and Shervais, J.W., eds., *Ophiolites, Arcs, and Batholiths: A Tribute to Cliff Hopson*: Geological Society of America Special Paper 438, p. 1–101, [https://doi.org/10.1130/2008.2438\(01\)](https://doi.org/10.1130/2008.2438(01)).
- Hoskin, P.W.O., and Ireland, T.R., 2000, Rare earth element chemistry of zircon and its use as a provenance indicator: *Geochimica et Cosmochimica Acta*, v. 28, p. 627–630, [https://doi.org/10.1130/0091-7613\(2000\)28<627:REECOZ>2.0.CO;2](https://doi.org/10.1130/0091-7613(2000)28<627:REECOZ>2.0.CO;2).
- Hoskin, P.W.O., and Schaltegger, U., 2003, The composition of zircon and igneous and metamorphic petrogenesis: Reviews in Mineralogy and Geochemistry, v. 53, p. 27–62, <https://doi.org/10.2113/0530027>.
- Ingersoll, R.V., 1979, Evolution of the Late Cretaceous forearc basin, northern and central California: *Geological Society of America Bulletin*, v. 90, p. 813–826, [https://doi.org/10.1130/0016-7606\(1979\)90<813:EOTLCF>2.0.CO;2](https://doi.org/10.1130/0016-7606(1979)90<813:EOTLCF>2.0.CO;2).
- Ingersoll, R.V., 1983, Petrofacies and provenance of late Mesozoic forearc basin: Northern and central California: *American Association of Petroleum Geologists Bulletin*, v. 67, p. 1125–1142.
- Ingersoll, R.V., 2000, Models for origin and emplacement of Jurassic ophiolites of northern California, *in* Dilek, Y., Moores, E.M., Elthon, D., and Nicolas, A., eds., *Ophiolites and Oceanic Crust: New Insights from Field Studies and the Ocean Drilling Program*: Geological Society of America Special Paper 349, p. 395–402, <https://doi.org/10.1130/0-8137-2349-3.395>.
- Ingersoll, R.V., 2008, Subduction-related sedimentary basins of the U.S. Cordillera, *in* Miall, A.D., ed., *The Sedimentary Basins of the United States and Canada: Sedimentary Basins of the World Volume 5* [Hsu, K.J., ed.]: Amsterdam, Netherlands, Elsevier, p. 395–428, [https://doi.org/10.1016/S1874-5997\(08\)00011-7](https://doi.org/10.1016/S1874-5997(08)00011-7).
- Irwin, W.P., and Wooden, J.L., 2001, Map Showing Plutons and Accreted Terranes of the Sierra Nevada, California with a Tabulation of U/Pb Isotopic Ages: U.S. Geological Survey Open-File Report 2001-229, scale 1:100,000, <https://doi.org/10.3133/ofr01229>.
- Kirkland, C.L., Smithies, R.H., Taylor, R.J.M., Evans, N., and McDonald, B., 2015, Zircon Th/U ratios in magmatic environs: *Lithos*, v. 212–215, p. 397–414, <https://doi.org/10.1016/j.lithos.2014.11.021>.
- Kistler, R.W., and Peterman, Z.E., 1973, Variations in Sr, Rb, K, Na, and initial $^{87}\text{Sr}/^{86}\text{Sr}$ in Mesozoic granitic rocks and intruded wall rocks in central California: *Geological Society of America Bulletin*, v. 84, p. 3489–3512, [https://doi.org/10.1130/0016-7606\(1973\)84<3489:VISRKN>2.0.CO;2](https://doi.org/10.1130/0016-7606(1973)84<3489:VISRKN>2.0.CO;2).
- Kistler, R.W., Chappell, B.W., Peck, D.L., and Bateman, P.C., 1986, Isotopic variation in the Tuolumne intrusive suite, central Sierra Nevada, California: Contributions to Mineralogy and Petrology, v. 94, p. 205–220, <https://doi.org/10.1007/BF00592937>.
- Klemetti, E.W., Lackey, J.S., and Starnes, J., 2014, Magmatic lulls in the Sierra Nevada captured in zircon from rhyolite of the Mineral King pendant, California: *Geosphere*, v. 10, no. 1, p. 66–79, <https://doi.org/10.1130/GES00920.1>.
- Lackey, J.S., Cecil, M.R., Windham, C.J., Frazer, R.E., Bindeman, I.N., and Gehrels, G.E., 2012, The Fine Gold intrusive suite: The roles of basement terranes and magma source development in the Early Cretaceous Sierra Nevada batholith: *Geosphere*, v. 8, p. 292–313, <https://doi.org/10.1130/GES00745.1>.
- Linn, A.M., DePaolo, D.J., and Ingersoll, R.V., 1991, Nd-Sr isotopic provenance analysis of Upper Cretaceous Great Valley fore-arc sandstones: *Geology*, v. 19, p. 803–806, [https://doi.org/10.1130/0091-7613\(1991\)019<0803:NSIPAO>2.3.CO;2](https://doi.org/10.1130/0091-7613(1991)019<0803:NSIPAO>2.3.CO;2).
- Ludwig, K.R., 2008, Isoplot 3.60: Berkeley Geochronology Center Special Publication 4, 77 p.
- Mansfield, C.F., 1979, Upper Mesozoic subsea fan deposits in the southern Diablo Range, California; record of the Sierra Nevada magmatic arc: *Geological Society of America Bulletin*, v. 90, p. 1025–1046, [https://doi.org/10.1130/0016-7606\(1979\)90<1025:UMSFDI>2.0.CO;2](https://doi.org/10.1130/0016-7606(1979)90<1025:UMSFDI>2.0.CO;2).
- Martin, M.W., and Clemens-Knott, D., 2015, Detrital-zircon record of the early Mesozoic southwestern Sierra Nevada arc preserved in Lower Cretaceous intra-arc and forearc deposits of central California, USA, *in* Anderson, T.H., Didenko, A.N., Johnson, C.L., Khanchuk, A.I., and MacDonald, J.H., Jr., eds., *Late Jurassic Margin of Laurasia—A Record of Faulting Accommodating Plate Rotation*: Geological Society of America Special Paper 513, p. 269–284, [https://doi.org/10.1130/2015.2513\(06\)](https://doi.org/10.1130/2015.2513(06)).
- May, J.C., and Hewitt, R.L., 1948, The basement complex in well samples from Sacramento and San Joaquin Valleys, California: *California Division of Mines and Geology Journal*, v. 44, p. 129–158.
- Mazdab, F.K., and Wooden, J.L., 2006, Trace element analysis in zircon by ion microprobe (SHRIMP-RG): Technique and applications: *Geochimica et Cosmochimica Acta*, v. 70, p. A405, <https://doi.org/10.1016/j.gca.2006.06.817>.
- Memeti, V., Gehrels, G.E., Paterson, S.R., Thompson, J.M., Mueller, R.M., and Pignotta, G.S., 2010, Evaluating the Mojave–Snow Lake fault hypothesis and origins of central Sierran metasedimentary pendant strata using detrital zircon provenance analyses: *Lithosphere*, v. 2, p. 341–360, <https://doi.org/10.1130/L58.1>.
- Mitchell, C., Graham, S.A., and Suek, D.H., 2010, Subduction complex uplift and exhumation and its influence on Maastriachian forearc stratigraphy in the Great Valley Basin, northern San Joaquin Valley, California: *Geological Society of America Bulletin*, v. 122, p. 2063–2078, <https://doi.org/10.1130/B30180.1>.
- Monteleone, B.D., Baldwin, S.L., Webb, L.E., Fitzgerald, P.G., Grove, M., and Schmitt, A.K., 2007, Late Miocene–Pliocene eclogite facies metamorphism, D'Entrecasteaux Islands, SE Papua New Guinea: *Journal of Metamorphic Geology*, v. 25, no. 2, p. 245–265, <https://doi.org/10.1111/j.1525-1314.2006.00685.x>.
- Moxon, I.W., 1990, Stratigraphic and Structural Architecture of the San Joaquin–Sacramento Basin [Ph.D. thesis]: Stanford, California, Stanford University, 371 p.
- Ojakangas, R.W., 1968, Cretaceous sedimentation, Sacramento Valley, California: *Geological Society of America Bulletin*, v. 79, p. 973–1008, [https://doi.org/10.1130/0016-7606\(1968\)79\[973:CSSVC\]2.0.CO;2](https://doi.org/10.1130/0016-7606(1968)79[973:CSSVC]2.0.CO;2).
- Paterson, S.R., and Ducea, M.N., 2015, Arc magmatic tempos: Gathering the evidence: *Elements*, v. 11, p. 91–98, <https://doi.org/10.2113/gselements.11.2.91>.
- Rose, R.L., and Colburn, I.P., 1963, Geology of the east-central part of the Priest Valley Quadrangle, California, *in* *Geology of the Salinas Valley and the San Andreas Fault*: American Association of Petroleum Geologists and Society of Economic Paleontologists and Mineralogists, Pacific Sections, Annual Spring Field Trip Guidebook: Los Angeles, California, Pacific Section, American Association of Petroleum Geologists, p. 38–45.
- Russel, J.S., Baum, S.L., and Watkins, R., 1986, Late Coniacian to early Campanian clastic shelf deposits and molluscan assemblages of the northeastern Sacramento Valley, California, *in* Abbott, P.L., ed., *Cretaceous Stratigraphy, Western North America*: Society of Economic Paleontologists and Mineralogists, Pacific Section Field Trip Guidebook 46, p. 179–196.
- Saleeby, J., 2007, The western extent of the Sierra Nevada batholith in the Great Valley basement and its significance in underlying mantle dynamics: *Eos (Transactions, American Geophysical Union)*, v. 88, no. 52, abstract T31E–02.
- Saleeby, J.B., 2011, Geochemical mapping of the Kings-Kaweah ophiolite belt, southwestern Sierra Nevada, foothills—Evidence for progressive mélange formation in a large offset transform-subduction initiation environment, *in* Wakabayashi, J., and Dilek, E., eds., *Mélanges: Processes of Formation and Societal Significance*: Geological Society of America Special Paper 480, p. 31–73, [https://doi.org/10.1130/2011.2480\(02\)](https://doi.org/10.1130/2011.2480(02)).
- Saleeby, J.B., and Busby-Spera, C., 1992, Early Mesozoic tectonic evolution of the western U.S. Cordillera, *in* Burchfiel, B.C., Lipman, P.W., and Zoback, M.L., eds., *The Cordilleran Orogen: Continental U.S.: Boulder, Colorado, Geological Society of America, The Geology of North America*, v. G-3, p. 107–138, <https://doi.org/10.1130/DNAG-GNA-G3.107>.
- Saleeby, J.B., and Dunne, G., 2015, Temporal and tectonic relations of early Mesozoic arc magmatism, southern Sierra Nevada, California, *in* Anderson, T.H., Didenko, A.N., Johnson, C.L., Khanchuk, A.I., and MacDonald, J.H., Jr., eds., *Late Jurassic Margin of Laurasia—A Record of Faulting Accommodating Plate Rotation*: Geological Society of America Special Paper 513, p. 223–268, [https://doi.org/10.1130/2015.2513\(05\)](https://doi.org/10.1130/2015.2513(05)).
- Saleeby, J.B., Sams, D.B., and Kistler, R.W., 1987, U/Pb zircon, strontium, and oxygen isotopic and geochronological study of the southernmost Sierra Nevada batholith, California: *Journal of Geophysical Research*, v. 92, no. B10, p. 10,443–10,466, <https://doi.org/10.1029/JB092iB10p10443>.
- Saleeby, J.B., Shaw, H.F., Niemeyer, S., Edelman, S.H., and Moores, E.M., 1989, U/Pb, Sm/Nd and Rb/Sr geochronological and isotopic study of northern Sierra Nevada ophiolitic assemblages, California: Contributions to Mineralogy and Petrology, v. 102, p. 205–220, <https://doi.org/10.1007/BF00375341>.
- Saleeby, J.B., Ducea, M., and Clemens-Knott, D., 2003, Production and loss of high-density batholithic root, southern Sierra Nevada, California: *Tectonics*, v. 22, 1064, <https://doi.org/10.1029/2002TC001374>.
- Sano, Y., Terada, K., and Fukuoka, T., 2002, High mass resolution ion microprobe analysis of rare earth elements in silicate glass, apatite and zircon: Lack of matrix dependency: *Chemical Geology*, v. 184, p. 217–230, [https://doi.org/10.1016/S0009-2541\(01\)00366-7](https://doi.org/10.1016/S0009-2541(01)00366-7).
- Schilling, F.A., Jr., 1962, *The Upper Cretaceous Stratigraphy of the Pacheco Pass Quadrangle, California* [Ph.D. thesis]: Stanford, California, Stanford University, 153 p.
- Schmitt, A.K., Konrad, K., Andrews, G.D., Horie, K., Brown, S.R., Koppers, A.A., Pecha, M., Busby, C.J., and Tamura, Y., 2018, $^{40}\text{Ar}/^{39}\text{Ar}$ ages and zircon petrochronology for the rear arc of the Izu-Bonin-Marianas intra-oceanic subduction zone: *International Geology Review*, v. 60, p. 956–976, <https://doi.org/10.1080/00206814.2017.1363675>.
- Schweickert, R.A., 2015, Jurassic evolution of the western Sierra Nevada metamorphic province, *in* Anderson, T.H., Didenko, A.N., Johnson, A.N., Khanchuk, A.I., and MacDonald, J.H., Jr., eds., *Late Jurassic Margin of Laurasia—A Record of Faulting Accommodating Plate Rotation*: Geological Society of America Special Paper 513, p. 299–358, [https://doi.org/10.1130/2015.2513\(08\)](https://doi.org/10.1130/2015.2513(08)).
- Schweickert, R.A., and Cowan, D.S., 1975, Early Mesozoic tectonic evolution of the western Sierra Nevada, California: *Geological Society of America Bulletin*, v. 86, p. 1329–1336, [https://doi.org/10.1130/0016-7606\(1975\)86<1329:EMTEOT>2.0.CO;2](https://doi.org/10.1130/0016-7606(1975)86<1329:EMTEOT>2.0.CO;2).
- Seiders, V.M., 1983, Correlation and provenance of Upper Mesozoic chert-rich conglomerate of California: *Geological Society of America Bulletin*, v. 94, p. 875–888, [https://doi.org/10.1130/0016-7606\(1983\)94<875:CAPOUM>2.0.CO;2](https://doi.org/10.1130/0016-7606(1983)94<875:CAPOUM>2.0.CO;2).
- Sharman, G.R., Graham, S.A., Grove, M., Kimbrough, D.L., and Wright, J.E., 2015, Detrital zircon provenance of the Late Cretaceous–Eocene California forearc: Influence of Laramide low-angle subduction on sediment dispersal and paleogeography: *Geological Society of America Bulletin*, v. 127, p. 38–60, <https://doi.org/10.1130/B31065.1>.
- Shervais, J.W., Murchy, B.L., Kimbrough, D.L., Renne, P.R., and Hanan, B., 2005, Radioisotopic and biostratigraphic age relations in the Coast Range ophiolite, northern California: Implications for the tectonic evolution of the western Cordillera: *Geological Society of America Bulletin*, v. 117, p. 633–653, <https://doi.org/10.1130/B25443.1>.
- Short, P.F., and Ingersoll, R.V., 1990, Petrofacies and provenance of the Great Valley Group, southern Klamath Mountains and northern Sacramento Valley, *in* Ingersoll, R.V., and Nilsen, T.H., eds., *Sacramento Valley Symposium and Guidebook*: Pacific Section, Society of Economic Paleontologists and Mineralogists (SEPM), Book 65, p. 39–52.
- Stern, T.W., Bateman, P.C., Morgan, B.A., Newell, M.F., and Peck, D.L., 1981, Isotopic U-Pb Ages of Zircons from the Granitoids of the Central Sierra Nevada, California: *U.S. Geological Survey Professional Paper 1185*, 17 p., <https://doi.org/10.3133/pp1185>.
- Suchocki, R.K., 1984, Facies history of the Upper Jurassic–Lower Cretaceous Great Valley Sequence: Response to structural development of an outer-arc basin: *Journal of Sedimentary Petrology*, v. 54, p. 170–191.
- Surpless, K.D., 2014, Geochemistry of the Great Valley Group: An integrated provenance record: *International Geology Review*, v. 57, no. 5–8, p. 747–766.

- Surpless, K.D., and Augsburger, G.A., 2009, Provenance of the Pythian Cave conglomerate, northern California: Implications for mid-Cretaceous paleogeography of the U.S. Cordillera: *Cretaceous Research*, v. 30, p. 1181–1192, <https://doi.org/10.1016/j.cretres.2009.05.005>.
- Surpless, K.D., Graham, S.A., Covault, J.A., and Wooden, J.L., 2006, Does the Great Valley Group contain Jurassic strata? Reevaluation of the age and early evolution of a classic forearc basin: *Geology*, v. 34, p. 21–24, <https://doi.org/10.1130/G21940.1>.
- van de Kamp, P.C., and Leake, B.E., 1985, Petrography and geochemistry of feldspathic and mafic sediments of the northeastern Pacific margin: *Transactions of the Royal Society of Edinburgh—Earth Sciences*, v. 76, no. 4, p. 411–449, <https://doi.org/10.1017/S0263593300010646>.
- Wakabayashi, J., 2015, Anatomy of a subduction complex: Architecture of the Franciscan Complex, California, at multiple length and time scales: *International Geology Review*, v. 57, p. 669–746, <https://doi.org/10.1080/00206814.2014.998728>.
- Walker, B.A., Grunder, A.L., and Wooden, J.L., 2010, Organization and thermal maturation of long-lived arc systems: Evidence from zircons at the Aucanquilcha volcanic cluster, northern Chile: *Geology*, v. 38, p. 1007–1010, <https://doi.org/10.1130/G31226.1>.
- Williams, T.A., 1997, Basin-Fill Architecture and Forearc Tectonics: Cretaceous Great Valley Group, Sacramento Basin, Northern California [Ph.D. thesis]: Stanford, California, Stanford University, 412 p.
- Williams, T.A., and Graham, S.A., 2013, Controls on forearc basin architecture from seismic and sequence stratigraphy of the Upper Cretaceous Great Valley Group, central Sacramento Basin, California: *International Geology Review*, v. 55, p. 2030–2059, <https://doi.org/10.1080/00206814.2013.817520>.
- Wright, J.E., and Wyld, S.J., 1986, Significance of xenocrystic Precambrian zircon contained within the southern continuation of the Josephine ophiolite, Devil's Elbow ophiolite remnant, Klamath Mountains, northern California: *Geology*, v. 14, p. 671–674, [https://doi.org/10.1130/0091-7613\(1986\)14<671:SOXPZC>2.0.CO;2](https://doi.org/10.1130/0091-7613(1986)14<671:SOXPZC>2.0.CO;2).
- Wright, J.E., and Wyld, S.J., 2007, Alternative tectonic model for Late Jurassic through Early Cretaceous evolution of the Great Valley Group, California, in Cloos, M., Carlson, W.D., Gilbert, M.C., Liou, J.G., and Sorenson, S.S., eds., *Convergent Margin Terranes and Associated Regions: A Tribute to W.G. Ernst*: Geological Society of America Special Paper 419, p. 81–95, [https://doi.org/10.1130/2007.2419\(04\)](https://doi.org/10.1130/2007.2419(04)).

MANUSCRIPT RECEIVED 20 DECEMBER 2018

REVISED MANUSCRIPT RECEIVED 23 APRIL 2019

MANUSCRIPT ACCEPTED 23 MAY 2019